
When Perplexity Lies: Generation-Focused Distillation of Hybrid Sequence Models

Juan Gabriel Kostelec
Huawei Zurich Research Center, Switzerland

juan.gabriel.kostelec@huawei.com

Xiang Wang
ACS Lab, Huawei Technologies

wangxiang224@huawei.com

Axel Laborieux
Huawei Zurich Research Center, Switzerland

axel.laborieux@huawei.com

Christos Sourmpis
Huawei Zurich Research Center, Switzerland

christos.sourmpis@h-partners.com

Guo Qinghai
ACS Lab, Huawei Technologies

guoqinghai@huawei.com

Abstract

Converting a pretrained Transformer into a more efficient hybrid model through distillation offers a promising approach to reducing inference costs. However, achieving high-quality generation in distilled models requires careful joint design of both the student architecture and the distillation process. Many prior distillation works evaluate downstream multiple-choice benchmarks by ranking candidate answers with log-likelihood rather than requiring autoregressive generation, which can obscure important differences in model quality. For example, we show that a 7B parameter distilled model that nearly matches its teacher to within 0.2 pp under log-likelihood scoring actually falls behind by 20.8 pp when the model must generate answers autoregressively.

We propose a Hybrid Kimi Delta Attention (Hybrid-KDA) architecture paired with GenDistill, a multi-stage distillation pipeline, and use generation-based evaluation throughout to guide design decisions. Applying this approach to Qwen3-0.6B, we systematically ablate six design axes: training objective, loss masking, training duration, dataset selection, parameter freezing, and architecture choice. We find that log-likelihood-based evaluation consistently underestimates the gap between teacher and student, and can in some cases reverse the ranking of design choices, meaning that conclusions drawn from perplexity-only evaluation may be misleading. Among the factors we study, dataset selection, completion-only masking, and freezing attention layers during post-training have the largest impact on generation quality.

Our best Hybrid-KDA model retains 86–90% of teacher accuracy on knowledge benchmarks while reducing KV cache memory by up to 75% and improving time-to-first-token by 2–4× at 128K-token contexts.

1 Introduction

Transformer-based language models dominate modern NLP due to their strong accuracy and scaling properties. However, self-attention incurs $\mathcal{O}(n^2)$ time and memory complexity in the sequence length n , and practical deployments additionally pay a linearly growing key-value (KV) cache cost during autoregressive inference.

In parallel, efficient sequence models with linear-time recurrent-style computation, including state space models (SSMs), have emerged as an attractive alternative. These architectures can offer linear-time processing and $\mathcal{O}(1)$ *per-step* memory growth during generation (i.e., no KV cache), enabling faster decoding and a smaller memory footprint in long-context settings (Gu & Dao, 2024; Yang et al., 2024a; 2025c; Dao & Gu, 2024).

Because training large transformers from scratch is computationally expensive (often on the order of trillions of tokens), a growing line of work studies *cross-architecture distillation*: transferring capabilities from a pretrained transformer teacher into a more efficient recurrent student (Wang et al., 2024; Bick et al., 2025a; 2024; Goldstein et al., 2025).

Despite encouraging results, prior methods for distilling Transformers into SSMs both optimize for and evaluate on perplexity, without targeting generation quality at any stage of the pipeline. While the broader NLP community has long recognized that perplexity is an imperfect proxy for generation quality, this gap takes on particular severity in cross-architecture distillation. The crux of the issue lies in how models are evaluated. *Perplexity-based* evaluation computes the log-likelihood of each candidate answer conditioned on the prompt and selects the highest-scoring option, testing whether the model *assigns high probability* to correct answers. *Generation-based* evaluation requires the model to produce answers autoregressively, after which outputs are typically parsed from an expected format or verified with task-specific criteria (e.g., exact-match answers or executable code), testing whether the model can *generate* correct answers. In this work, we use LM Evaluation Harness (Gao et al., 2024) for perplexity-based evaluation and EvalScope (ModelScope Team, 2024) for generation-based evaluation. The distinction is consequential because a model can rank correct answers highly without being able to generate them. To illustrate the severity of this discrepancy, we evaluate QRWKV6-7B-Instruct (Lin et al., 2025), distilled from Qwen2.5-7B-Instruct, under both evaluation protocols. Table 1 compares perplexity-based results reported by the original paper with our generation-based evaluation on the same benchmarks.

Table 1: Evaluation protocol gap for QRWKV6-7B-Instruct, distilled from Qwen2.5-7B-Instruct. PPL-based results are taken from the original paper; generation-based results are our evaluation using EvalScope. Both columns evaluate the *same model checkpoint*; only the evaluation protocol differs. On overlapping benchmarks, the average teacher–student gap jumps from **0.2 pp** (PPL) to **20.8 pp** (generation).

Model	PPL-based Evaluation				Generation-based Evaluation							
	ARC-E	ARC-C	HS	WG	ARC-E	ARC-C	HS	WG	GSM8K	HEval	IFEval	
Qwen2.5-7B-Instruct	81.5	55.0	80.5	71.4	91.9	87.7	82.3	66.2	90.2	85.4	71.4	
QRWKV6-7B-Instruct	81.4	56.3	79.0	71.1	75.2	62.4	49.9	57.5	17.4	31.7	46.6	

As Table 1 shows, the gap is severe: QRWKV6-7B-Instruct nearly matches its teacher under PPL-based evaluation (0.2 pp gap) yet falls behind by 20.8 pp under generation. This pattern is representative of the broader literature, where cross-architecture distillation pipelines typically report only log-likelihood-based results (Wang et al., 2024; Bick et al., 2025a; 2024; Goldstein et al., 2025). Recent works such as M1 (Wang et al., 2025) and MiniCPM-SALA (Team et al., 2026) address this through additional SFT and RL stages, but at substantial cost (e.g. 1T tokens for MiniCPM-SALA). We instead investigate the fundamental distillation choices themselves and how to maximize the generation quality of the distilled model without additional continual training. In this work, we propose a Hybrid Kimi Delta Attention (Hybrid-KDA) architecture paired with GenDistill, a multi-stage distillation pipeline designed around it, and use generation-based evaluation throughout to guide every design decision. We systematically investigate how both architectural choices and distillation recipe choices impact the student’s instruction-following and reasoning capabilities.

Our main contributions are:

- We demonstrate that perplexity-based evaluation is a systematically misleading proxy for generation quality in cross-architecture distillation, with the divergence appearing consistently across every design axis we study. This motivates generation-based evaluation as the primary protocol for this setting.

- We propose a Hybrid-KDA architecture paired with GenDistill, a multi-stage distillation pipeline incorporating beam-search-based attention layer selection and a generation-focused training recipe. We will release our model code and distilled checkpoints upon publication.
- Using generation-based evaluation, we systematically ablate six design axes (training objective, loss masking, training duration, parameter freezing, dataset selection, and architecture choice), yielding a concrete distillation recipe: KD with completion-only masking, teacher-aligned instruction data, and frozen attention layers.

2 Related Works

The computational demands of Transformer-based language models have motivated substantial research on converting pre-trained models to architectures with subquadratic complexity. Chronologically, this line of work first focused on fine-tuning-based approaches that directly modify attention mechanisms and continue training with standard language modeling objectives, and later expanded to distillation-based approaches that transfer knowledge from Transformer teachers to structurally different student models.

Early works focused on replacing the softmax attention layer with expressive linear kernels, followed by fine-tuning the resulting model for 1–40B tokens (Chen et al., 2024; Kostelec & Guo, 2025; Zhang et al., 2024; Mercat et al., 2024). Notably, LoLCats (Zhang et al., 2025) achieved conversion with as few as 40M tokens via a two-stage approach: 20M tokens for attention alignment followed by 20M tokens to train LoRA adapters to recover model performance. However, these methods still exhibited a performance gap, particularly on benchmarks such as MMLU.

More recent works have leveraged multi-stage distillation for model conversion and generally report substantially stronger student performance. For example, MOHAWK (Bick et al., 2024) introduced a three-stage pipeline that (i) aligns attention matrices, (ii) aligns attention-layer output hidden states, and (iii) performs full-model knowledge distillation. Similar pipelines were proposed by Wang et al. (2024) (initializing the student sequence mixer from teacher weights, adding additional DPO stages, and focusing on hybrid models), Bick et al. (2025a) (scaling MOHAWK to larger models), and Yang et al. (2025b) (distilling into a hybrid model with multi-head latent attention and Mamba layers). A concurrent work (Goldstein et al., 2025) proposed a highly efficient distillation process, using only 700M tokens while reporting state-of-the-art results on downstream tasks, however, they focused on purely recurrent models and have only evaluated with LM-evaluation harness (PPL-based).

One fundamental limitation of SSMS and linear-attention models is their fixed hidden-state size, which can significantly degrade performance on in-context retrieval tasks. Consequently, many works have explored hybrid models to mitigate this gap. Two directions are relevant here: intra-layer hybrids, which replace only a subset of attention heads within a layer with SSM heads, and inter-layer hybrids, which replace entire attention layers with SSM layers. Although intra-layer hybrids allow a finer-grained choice of which attention heads to keep and which to convert to SSMS (Zuo et al., 2025; Dong et al., 2025), they can increase system complexity and inference overhead, complicating distributed parallelism optimizations (Team et al., 2025). For inter-layer hybrids, the choice of which attention layers are kept intact is crucial, as some layers appear to be critical for retrieval performance (Bick et al., 2025b).

Prior approaches have selected attention layers uniformly (Lieber et al., 2025; De et al., 2024; Bick et al., 2024). SMART (Yang et al., 2025b) studied the sensitivity of each layer (measured by the reduction in teacher–student KL divergence) when swapping a linear layer with an attention layer, and then heuristically selected layers to maximize total sensitivity. PostNAS (Gu et al., 2025) used a complex search procedure, training a once-for-all supernet and using beam search to find the optimal K layers for specific downstream tasks. A concurrent approach proposed greedily adding attention layers back to a distilled fully linear model by measuring the KL divergence of the output logits between the resulting hybrid model and the original teacher model after distilling the teacher into the hybrid model (Li et al., 2026).

3 Background

3.1 Kimi Delta Attention

Linear attention as associative memory. Linear attention (Katharopoulos et al., 2020) replaces the softmax attention kernel with an outer-product update to a matrix-valued recurrent state $\mathbf{S}_t \in \mathbb{R}^{d_k \times d_v}$:

$$\mathbf{S}_t = \mathbf{S}_{t-1} + \mathbf{k}_t \mathbf{v}_t^\top, \quad \mathbf{o}_t = \mathbf{S}_t^\top \mathbf{q}_t. \quad (1)$$

\mathbf{S}_t serves as an associative memory that stores key-value associations. However, the purely additive update accumulates information without any forgetting, causing interference as the context grows.

The delta rule and Gated DeltaNet. DeltaNet (Schlag et al., 2021; Yang et al., 2024b) addresses this by interpreting the state update as online gradient descent on a per-token reconstruction loss $\mathcal{L}_t(\mathbf{S}) = \frac{1}{2} \|\mathbf{S}^\top \mathbf{k}_t - \mathbf{v}_t\|^2$, yielding a rank-1 corrective update:

$$\mathbf{S}_t = (\mathbf{I} - \beta_t \mathbf{k}_t \mathbf{k}_t^\top) \mathbf{S}_{t-1} + \beta_t \mathbf{k}_t \mathbf{v}_t^\top, \quad (2)$$

where β_t is a learned step size. This delta rule enables the memory to correct stale associations rather than merely accumulating them. Gated DeltaNet (GDN) (Yang et al., 2025c) further introduces a *scalar* forget gate $\alpha_t \in [0, 1]$, acting as weight decay on the memory:

$$\mathbf{S}_t = \alpha_t (\mathbf{I} - \beta_t \mathbf{k}_t \mathbf{k}_t^\top) \mathbf{S}_{t-1} + \beta_t \mathbf{k}_t \mathbf{v}_t^\top. \quad (3)$$

This provides a principled mechanism to control memory lifespan. However, GDN’s scalar gate applies a uniform decay rate across all feature dimensions, limiting the model’s ability to selectively retain or forget information at a fine-grained level.

Channel-wise gating in KDA. Kimi Delta Attention (KDA) (Team et al., 2025) refines GDN by replacing the scalar gate with a *channel-wise* (i.e., per-dimension) diagonal gate $\text{Diag}(\boldsymbol{\alpha}_t) \in \mathbb{R}^{d_k \times d_k}$, where each feature dimension maintains an independent forgetting rate:

$$\mathbf{S}_t = (\mathbf{I} - \beta_t \mathbf{k}_t \mathbf{k}_t^\top) \text{Diag}(\boldsymbol{\alpha}_t) \mathbf{S}_{t-1} + \beta_t \mathbf{k}_t \mathbf{v}_t^\top, \quad \mathbf{o}_t = \mathbf{S}_t^\top \mathbf{q}_t. \quad (4)$$

4 The GenDistill pipeline

Producing a high-quality distilled model requires jointly designing the student architecture and the distillation process. This section describes both components: the Hybrid-KDA student architecture (Section 4.1), including a beam-search method for selecting which layers retain softmax attention (Section 4.1.1), and the multi-stage distillation process that progressively aligns the student with the teacher (Section 4.2).

4.1 Student Model Architecture

To preserve the foundational knowledge acquired during pretraining, our student model inherits the majority of its architecture directly from the pretrained teacher model. Specifically, the vocabulary, embedding layers, layer normalizations, and multi-layer perceptrons (MLPs) are initialized from the teacher, while select attention layers are replaced with more efficient sequence mixers to improve inference efficiency. The choice of sequence mixers used in the student model is crucial for the success of the distillation pipeline, both in terms of final student model performance, as well as how efficiently we can distill the transformer into the new architecture. Recent work has proposed several linear sequence mixers that maintain efficiency while improving model expressivity (e.g. Gated DeltaNet (Yang et al., 2025c), Kimi (Team et al., 2025), RWKV7 (Peng et al., 2025)). In this work, we focus on two linear architectures: Kimi Delta Attention (KDA) as our primary student mixer, and Mamba2 (Dao & Gu, 2024) as a baseline for comparison. We select Mamba2 because it is one of the most widely adopted SSMS and has been used as the student architecture in several prior distillation works (Phi-Mamba (Wang et al., 2024), Llama (Bick et al., 2025a)). We select KDA because of its strong reported performance.

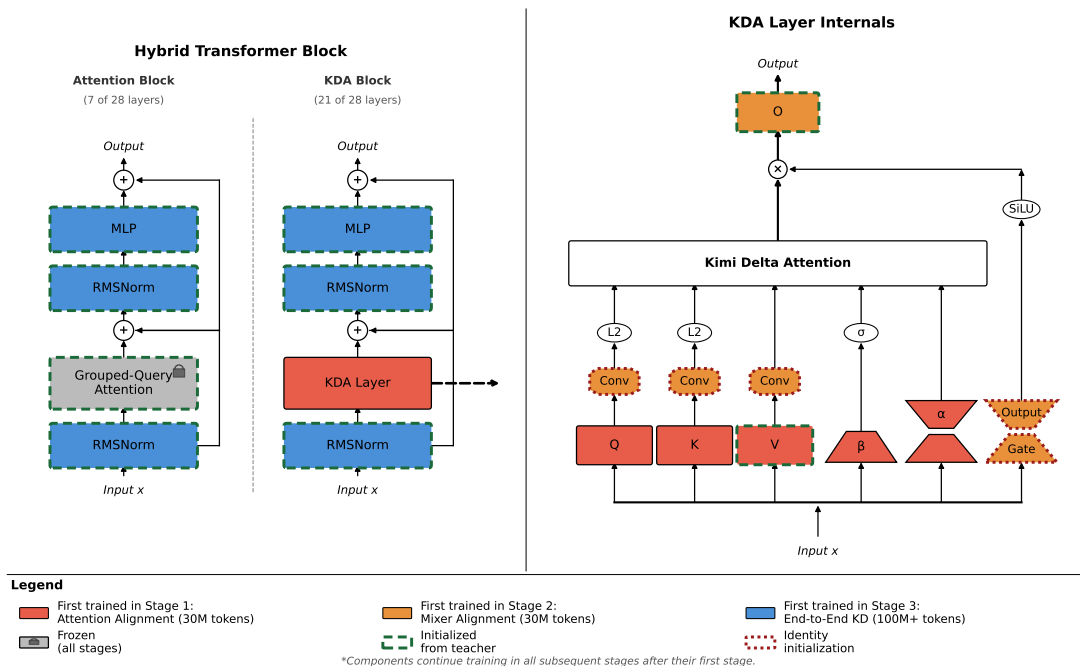


Figure 1: Architecture overview. **Left:** The two block types in the hybrid transformer: an Attention block (7 of 28 layers, frozen from the teacher) and a KDA block (21 of 28 layers). MLPs and layer norms are initialized from the teacher and trained only during end-to-end distillation (Stage 3). **Right:** Internal structure of the KDA layer. Fill colors indicate the earliest distillation stage in which each component begins training; once introduced, components continue training in all subsequent stages. Green dashed borders denote initialization from teacher weights; dark-red dotted borders denote identity initialization; the absence of a custom border denotes random initialization.

Additionally, there are several smaller architectural choices that have also proven important for a good and efficient distillation process. We enumerate them here, while an ablation is available in Appendix C. Similar to Bick et al. (2024), we observe that removing the output norm in the SSM improves the distillation process. We also use identity initialization of the short convolutions and the output gating in the Kimi layer, however, contrary to the findings in Team et al. (2025), we find that using SiLU gating is better than using Sigmoid gates in the distillation setting. Since we are distilling from the Qwen3 model family (Yang et al., 2025a), which uses QK norms in the attention layer, we also keep normalization of QK values in the Kimi layer¹.

4.1.1 Attention layer selection

In hybrid architectures, the selection of which layers retain softmax attention versus those replaced with linear alternatives significantly impacts model performance. While certain attention heads appear universally important for in-context retrieval (Bick et al., 2025b), our initial experiments revealed that optimal layer selection is more task-dependent.

Greedy layer selection may yield suboptimal configurations, as it fails to account for interactions between layers. To address this limitation, we employ beam search to explore layer combinations more thoroughly, similar to the approach in PostNAS (Gu et al., 2025). However, unlike PostNAS, we avoid training an extensive supernet by leveraging only the pretrained teacher model and a fully linear student model (comprising Kimi layers) obtained through our distillation pipeline.

¹We use L2 normalization without learnable scales, following the Kimi Delta Attention layer implementation in Yang & Zhang (2024).

Our search procedure, *Beam Search (Add)*, initializes from the fully linear student and iteratively restores attention layers from the teacher, retaining at each step the configurations that achieve the lowest perplexity. To account for task dependence, we evaluate perplexity on three complementary datasets: (i) a synthetic associative recall (AR) task that probes in-context retrieval, (ii) C-EVAL for Chinese language understanding, and (iii) FineWeb-EDU for general language modeling, and select layers based on the average across all three. The resulting layer selections and a detailed comparison of alternative selection strategies are provided in Appendix D.

4.2 Distillation Stages

GenDistill uses a multi-stage distillation process designed to progressively align the hybrid student model with the Transformer teacher. Direct end-to-end distillation can be inefficient under architectural mismatch, so we follow the bottom-up multi-stage blueprint of MOHAWK (Bick et al., 2024), with Stage 1 adapted to KDA by aligning hidden states rather than attention logits (KDA cannot efficiently materialize the full $N \times N$ attention matrix). We then perform end-to-end KD in Stage 3, separating pretraining-data distillation (Stage 3a) from instruction-tuning distillation (Stage 3b). We report generation-based evaluation alongside perplexity to capture quality differences that are not visible under likelihood-only protocols. Overall, using KDA as the student mixer allows us to operate at a smaller total token budget ($\sim 800\text{M}$) than prior multi-stage distillation pipelines (MOHAWK: $\sim 3\text{B}$; Llama: $\sim 8\text{B}$ (Bick et al., 2025a)). The pipeline consists of three main stages: (1) attention mechanism initialization and alignment, (2) block-wise hidden state alignment, and (3) end-to-end knowledge distillation for error correction and task adaptation.

4.2.1 Stage 1: Initialization and Attention Matrix Alignment

The student model inherits the embedding, normalization, and MLP layers directly from the teacher. For the sequence mixers, we replace specific attention layers with Kimi Delta Attention (KDA) layers. We initialize the Value (V) and Output (O) projections of the KDA layers using the corresponding weights from the teacher, exploiting the architectural similarity, see Figure 1. However, we find that initializing the Query (Q) and Key (K) projections from the teacher does not necessarily improve the training, and are thus initialized randomly.

While MOHAWK (Bick et al., 2024) aligns the full attention logits to approximate the teacher’s attention patterns, KDA cannot efficiently materialize the full $N \times N$ attention matrix. Instead, we minimize the L2 distance between the hidden states of the attention layers of the teacher and student. Only the Q and K projections are trained. We use a filtered subset of FineWeb-EDU and FineWeb-Edu-Chinese-2.1 (score ≥ 4)², training for 30M tokens with a sequence length of 2048. We employ a warmup-stable-decay learning rate schedule (max LR $5e - 4$, 10% warmup). Samples are packed into fixed sequence lengths with cross-document masking (Zuo et al., 2025).

4.2.2 Stage 2: Block-wise Hidden State Alignment

The second stage aligns the feature representations of the student and teacher blocks independently. We minimize the L2 distance between the outputs of the student’s mixer block and the teacher’s attention block. In this stage, all weights within the sequence mixer are trainable, while LayerNorms remain frozen as they are initialized from the teacher. We train for another 30M tokens using the same dataset and schedule as Stage 1, but with a reduced learning rate ($1e - 4$).

Crucially, we find that this two-step alignment (Stage 1 followed by Stage 2) is superior to training the mixer all at once or initializing all weights from the teacher. Skipping Stage 1 results in significant perturbations to the initialized V and O weights, destabilizing the training. By the end of this stage, after only 60M tokens, the student model achieves a validation perplexity of ~ 25 without any end-to-end training. This provides a stronger starting point than prior initialization methods, as KDA’s higher expressivity yields lower perplexity (e.g., MOHAWK (Bick et al., 2024) requires 240M tokens to reach ~ 1000 PPL, while Llama (Bick et al., 2025a) extends this stage to 3B tokens).

²Datasets: Fineweb-EDU (score ≥ 4) and Fineweb-Edu-Chinese-2.1 (filtered subset).

4.2.3 Stage 3: End-to-End Knowledge Distillation

Block-wise alignment treats layers independently, leading to error accumulation when layers are composed during inference. To address this and recover coherent text generation capabilities, we perform end-to-end knowledge distillation (KD). We minimize the forward KL divergence between the teacher and student output logits. We freeze the attention layers and input embeddings, training all other parameters.

This stage is divided into two phases. First, we distill on the pretraining dataset to couple the layers and smooth internal representations (Stage 3a; we ablate the token budget in Section 6.2). Second, to adapt the model for instruction following, we switch to the AM-Qwen3-Distilled dataset (Tian et al., 2025)³ (Stage 3b; we ablate design choices in Section 6.4). We increase the sequence length to 4096 and use a learning rate of $2.5e - 5$. For Stage 3b we ablate full-sequence versus completion-only masking; in practice, completion-only masking better targets the distillation signal to the answer tokens. Prior multi-stage distillation pipelines typically stop after pretraining-style distillation and do not include a dedicated instruction-tuning KD stage (e.g., MOHAWK; RADLADS (Goldstein et al., 2025)), and Llama uses a different post-training data recipe (Bick et al., 2025a). This separation ensures the student first recovers general language modeling capabilities over a broad distribution before learning also instruction-following and reasoning abilities from the teacher.

5 Evaluation Setup

Having described the Hybrid-KDA architecture and GenDistill pipeline (Section 4), we now turn to evaluation. A central design choice in our evaluation is the use of *two complementary protocols* that, as we show in Section 6.4, can tell contradictory stories about model quality:

- **Generation-based evaluation:** The model generates answers autoregressively. Responses are scored against reference answers. This protocol tests whether the model can *produce* correct answers, i.e. the practical use case for deployed models.
- **Log-likelihood ranking on multiple-choice tasks:** The model scores each candidate answer by its log-likelihood conditioned on the prompt, and the highest-scoring candidate is selected. This protocol tests whether the model assigns high probability to correct answers, which can diverge substantially from generation quality.

In our implementation, we use EvalScope ModelScope Team 2024 for generation-based evaluation and LM Evaluation Harness Gao et al. 2024 primarily for the log-likelihood-based multiple-choice evaluations.

Benchmarks. We evaluate on short-context benchmarks across five categories: **language modeling** (LAMBADA (Paperno et al., 2016)); **common sense** (HellaSwag (Zellers et al., 2019), WinoGrande (Sakaguchi et al., 2021), PIQA (Bisk et al., 2020)); **knowledge** (MMLU-Redux⁴ (Gema et al., 2025), C-Eval (Huang et al., 2023), CMMLU (Li et al., 2024)); **reasoning** (ARC (Clark et al., 2018), BBH (Suzgun et al., 2023), GSM8k (Cobbe et al., 2021), HumanEval (Chen et al., 2021)); and **instruction following** (IFEval (Zhou et al., 2023)). We evaluate tasks in both frameworks where available to analyze evaluation discrepancies⁵. We additionally evaluate long-context quality using LongBench (Bai et al., 2024) and the NIAH-single subtasks from RULER (Hsieh et al., 2024)

³<https://huggingface.co/datasets/a-m-team/AM-Qwen3-Distilled>

⁴We use MMLU-Redux (Gema et al., 2025) for generation-based evaluation (EvalScope), as it corrects a number of erroneous questions identified in the original MMLU. For perplexity-based evaluation (LM Evaluation Harness), we use the standard MMLU, since MMLU-Redux is only available in a generative format in that framework. The two benchmarks are tightly correlated in terms of performance.

⁵For BBH, HumanEval, GSM8K the performance on the lm-evaluation-harness was trivially low, around 0, which is likely an issue with the task setup, so we do not report these tasks in the lm-evaluation harness framework.

6 Results

We first present the main results of our best GenDistill configuration, comparing architectures and quantifying efficiency gains (Section 6.1). We then systematically ablate the factors driving these results: pretraining distillation (Section 6.2), post-training dataset selection (Section 6.3), training objective, masking, and duration (Section 6.4), and parameter freezing (Section 6.5).

6.1 Architecture comparison

We begin by comparing the architectures produced by the full GenDistill pipeline, evaluating how the choice of sequence mixer (KDA vs. Mamba2) and the retention of attention layers (Hybrid vs. Pure) affect downstream generation quality. To isolate architectural effects, we change only the sequence mixer and whether attention layers are retained, while keeping all other hyperparameters fixed. We include Mamba2 as a baseline because it is one of the most widely adopted SSMS and has been used in prior distillation work (Phi-Mamba, Llama). The design choices behind the pipeline (i.e. pretraining budget, dataset, objective, and parameter freezing) are ablated in Sections 6.2–6.5. Full training and configuration details are provided in Appendix B.

Table 2: Comparison of distilled architectures (generation-based evaluation, EvalScope). “Hybrid” models retain (the selected) 7 attention layers, “Pure” models use 0. Results are averaged over 3 evaluation seeds. Best student result per column in **bold**.

Model	Knowledge			Common Sense		Reasoning				IF	
	C-Eval	MMLU-R	CMMLU	WG	HS	ARC-E	ARC-C	BBH	GSM8K	HEval	IFEval
<i>Teacher (Qwen3-0.6B)</i>	42.9	46.1	45.2	51.2	39.0	70.8	55.0	27.4	57.5	35.3	57.1
Pure KDA	26.2	29.4	35.1	38.6	20.3	47.9	33.9	5.4	22.8	12.8	34.7
Pure Mamba	17.9	18.0	25.2	24.7	17.3	20.7	19.9	8.4	8.3	6.1	28.2
Hybrid Mamba	37.8	38.6	37.1	50.1	29.0	63.3	46.2	12.1	28.3	11.2	43.7
Hybrid KDA	38.2	40.3	38.7	50.7	30.0	63.5	48.4	18.9	34.5	19.9	46.7

Table 2 shows that retaining a subset of attention layers is critical: Hybrid models consistently outperform their Pure counterparts, with the largest separations on multi-step reasoning benchmarks (BBH, GSM8K). This pattern supports our design choice to preserve attention for compositional computation while using linear mixers for the majority of layers. Comparing the two sequence mixers, KDA consistently outperforms Mamba2, with the advantage most pronounced on the hardest reasoning and code-generation tasks. Perplexity-based evaluation results are reported in Appendix J (Table 19); they preserve the same architecture ranking but substantially compress the performance gaps.

Overall, the best Hybrid-KDA student retains 86–99% of teacher accuracy on knowledge and common-sense tasks, confirming that the majority of the teacher’s factual and linguistic knowledge transfers successfully. The largest remaining gaps appear on multi-step reasoning (BBH: 69%, GSM8K: 60%) and code generation (HumanEval: 56%), tasks that require extended autoregressive coherence. Closing these gaps likely requires either larger token budgets, on-policy distillation, or dedicated RL training.

6.1.1 Efficiency Analysis

A primary motivation for adopting hybrid architectures is to alleviate the inference bottlenecks of standard Transformers, namely, the quadratic prefill complexity and the rapidly growing KV cache memory at long contexts. Figure 2 illustrates how our hybrid models resolve these issues. By replacing attention layers with state space models, the hybrid architectures reduce KV cache memory by up to 75%⁶, allowing for 4× larger batch sizes or sequence lengths. Although SSM prefill ($\mathcal{O}(n)$) experiences slight kernel overhead on short sequences, it scales linearly and eventually becomes 2–4× faster than attention ($\mathcal{O}(n^2)$) at 128K tokens. Decoding throughput is similarly stable: while KDA is initially ~30% slower than Transformers at short

⁶Replacing attention with KDA or Mamba2 slightly *increases* total parameter count (613M vs. 596M non-embedding) due to extra gating and convolution parameters; the efficiency gains stem from $\mathcal{O}(n)$ vs. $\mathcal{O}(n^2)$ complexity scaling, not parameter reduction.

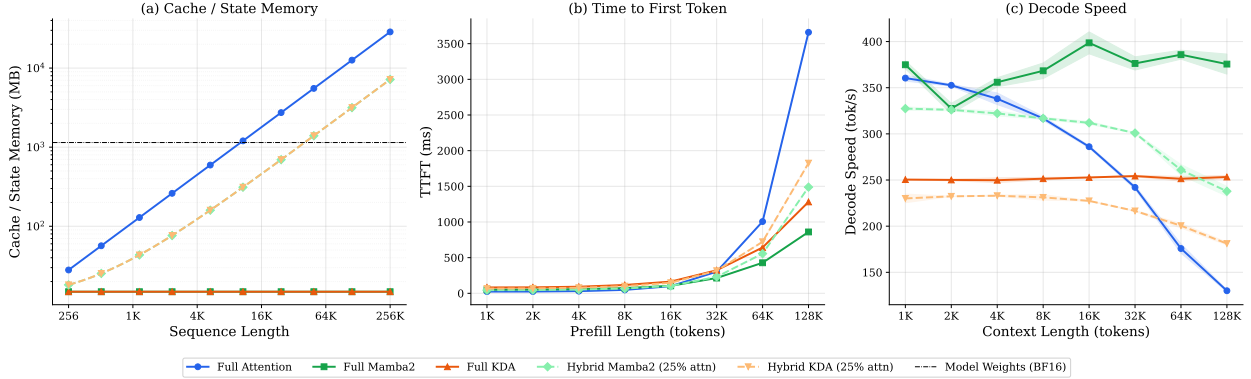


Figure 2: Inference efficiency comparison (single GPU, batch size 1). **(a)** Memory usage: SSMs use constant $\mathcal{O}(1)$ state, reducing hybrid memory footprint by up to 75%. **(b)** Time to First Token: Linear SSM scaling yields 2–4 \times speedups at long contexts (128K) despite short-context overhead. **(c)** Decode speed: SSMs maintain constant throughput; KDA reaches parity with Transformers at 32K tokens.

contexts, it achieves parity by 32K tokens. When evaluating throughput under GPU saturation (sweeping batch sizes until OOM; see Appendix K), hybrid models achieve up to 5 \times the teacher’s peak throughput at 128K tokens by successfully fitting larger batches.

6.2 Distilling on pretraining data

Prior work on efficient distillation mainly distilled on pre-training data alone (Goldstein et al., 2025). We thus first assess the impact of the amount of pretraining data (Stage 3a). We vary the Stage 3a token budget while holding the instruction-tuning stage (Stage 3b) fixed, so the student always learns the chat format and basic instruction-following behavior.⁷ Figure 3 confirms that increasing the Stage 3a budget monotonically reduces held-out KL divergence, indicating better distributional alignment with the teacher. However, improved distributional alignment from a longer Stage 3a does not proportionally increase downstream generation performance after Stage 3b (Table 3). While a larger Stage 3a budget consistently improves likelihood/KL alignment, downstream metrics are less sensitive: PIQA and MMLU remain essentially unchanged, though ARC and Winogrande show modest gains. We thus fix the Stage 3a budget to 500M tokens for subsequent experiments, balancing stronger likelihood alignment with modest downstream improvements.

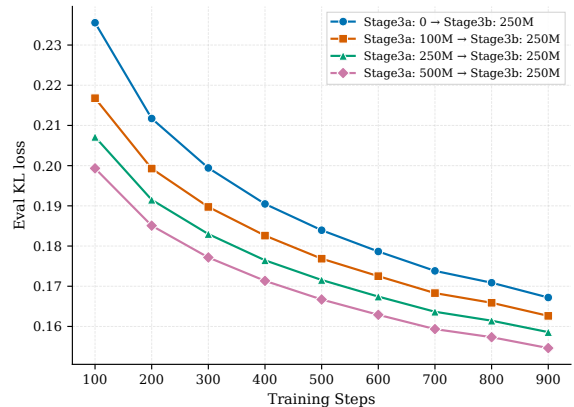


Figure 3: Held-out KL loss during Stage 3b for different Stage 3a token budgets.

6.3 Post-training dataset selection

After Stage 3a, the next decision is *which post training dataset* to use for Stage 3b. To isolate dataset effects, we fix the training setup (Hybrid-KDA student, KD objective, and a 500M-token budget) and vary only the Stage 3b data source among six post-training corpora: **AM-Qwen3-Distilled** (Tian et al., 2025), **SFTv3** (Wang et al., 2024), **Smoltalk2** (Bakouch et al., 2025), **OpenHermes 2.5** (Teknum, 2023), **Nemotron Post Training Dataset v1** (Nathawani et al., 2025), and **Chinese-Instruct** (Zhang, 2025).

⁷These experiments use an earlier configuration with 5 attention layers. We later adopted 7 attention layers to match the 1:3 attention-to-SSM ratio used in other hybrid models (Team et al., 2025). Since this ablation compares relative rankings of configurations rather than absolute scores, the conclusions transfer to the 7-layer setup.

Table 3: Stage 3a dataset size ablation: downstream results after Stage 3a (top, perplexity-based) and after Stage 3b (bottom, generation-based). We report accuracy for all tasks except LAMBADA, where we report perplexity (\downarrow).

Checkpoint		WG \uparrow	HS \uparrow	LAMBADA \downarrow	ARC-E \uparrow	ARC-C \uparrow	PIQA \uparrow	MMLU \uparrow
Stage 3a	Stage 3b							
<i>Teacher (Qwen3-0.6B)</i>		55.5	47.3	24.7	55.6	34.2	65.9	40.2
<i>After Stage 3a (LM Evaluation Harness, perplexity-based)</i>								
100M	–	54.3	44.3	38.8	53.8	32.0	65.9	38.3
250M	–	54.9	44.7	32.8	50.2	31.5	66.4	30.2
500M	–	54.7	45.0	31.7	54.9	32.3	65.9	36.0
<i>After Stage 3b (EvalScope, generation-based)</i>								
100M	250M	31.1	18.9	43.6	46.6	35.3	65.2	30.6
250M	250M	30.3	17.8	42.8	51.1	38.1	65.1	30
500M	250M	36.1	18.6	41.3	52.4	38.1	64.7	30.2

Table 4 shows that dataset selection is a major driver of generation quality. The effect size is not subtle: average performance ranges from 26.2% (Chinese-Instruct) to 46.9% (AM-Qwen3-Distilled), and individual tasks vary by as much as 30.5 percentage points on ARC-E and 23.8 pp on HellaSwag. Overall, the ranking aligns with the growing evidence that *teacher-aligned* instruction data is critical for effective distillation. Goldstein et al. (2025) emphasize the importance of distilling on data whose distribution closely matches the teacher’s training data, and Tian et al. (2025) show that the choice of teacher model used to generate instruction responses significantly impacts student quality, with responses curated from the same model family yielding the best results. AM-Qwen3-Distilled, which includes Qwen3-generated responses verified for correctness, aligns with both of these principles. We therefore use it as the default Stage 3b dataset in subsequent experiments.

Table 4: Effect of the Stage 3b dataset on downstream performance (generation-based evaluation). All runs use the same token budget (500M); Avg is the mean over the six benchmarks.

Distillation dataset	C-Eval [%]	ARC-E [%]	ARC-C [%]	HS [%]	WG [%]	MMLU-redux [%]	Avg [%]
SFTv3	39.1	64.3	47.8	24.8	40.4	40.5	42.8
Chinese-Instruct	18.0	34.9	25.8	16.4	37.8	24.3	26.2
AM-Qwen3-Distilled	39.8	65.4	49.3	37.2	48.9	40.8	46.9
Smoltalk2	37.9	63.8	46.3	33.2	50.0	37.9	44.9
Open Hermes	37.0	49.1	33.9	13.4	42.0	35.8	35.2
Nemotron Post Training v1	33.1	57.0	41.9	24.9	42.8	37.0	39.5

6.4 Stage 3b design choices

Initial experiments showed that naively extending Stage 3b training did not improve generation quality. We therefore systematically vary three axes: training objective (KD vs. SFT), loss masking strategy (full-sequence vs. completion-only), and training duration (250M, 500M, 750M tokens). Table 5 summarizes the results.

KD vs. SFT. The training objective strongly affects generation quality: KD is consistently performing better than SFT across generation benchmarks (Table 5; full results in Table 18), with its advantages most visible on reasoning, code generation, and instruction following. By contrast, SFT often appears competitive under perplexity-based evaluation, highlighting that next-token likelihood on post-training data is not a reliable proxy for answer generation quality.

Loss Scope. Which tokens contribute to the training loss matters as much as the objective itself. When the loss is computed over the full sequence, SFT can match or exceed KD on some benchmarks, especially those that emphasize language modeling (e.g. Lambada). By contrast, computing the loss only on completion tokens consistently improves generation quality for both objectives (Table 5), with KD benefiting more from

Table 5: Stage 3b ablation: training objective, masking strategy, and training duration. All runs use the Hybrid-KDA architecture with 7 attention layers. Generation-based results (EvalScope, left) and perplexity-based results (LM Evaluation Harness, right). Masking: P+C = full-sequence (prompt + completion); C = completion-only. Best student result per column in **bold**.

Objective	Mask	Tok.	Generation-based (EvalScope)									Perplexity-based (LM-eval)							
			WG	HS	ARC-E	ARC-C	C-Eval	MMLU-R	CMMLU	GSM8K	HEval	IFEval	WG	HS	ARC-E	ARC-C	PIQA	LAM.L	MMLU
<i>Teacher (Qwen3-0.6B)</i>			51.2	39.0	70.8	55.0	42.9	46.1	45.2	57.5	35.3	57.1	55.5	47.3	55.6	34.2	65.9	24.7	40.2
SFT	P+C	250M	46.1	24.1	54.4	39.4	32.0	29.3	22.9	26.1	2.4	26.2	55.9	47.3	54.4	32.4	65.6	21.2	40.5
SFT	P+C	500M	45.8	23.2	50.1	37.0	25.7	28.6	22.5	26.5	4.3	26.4	56.0	47.7	52.5	34.0	65.3	20.8	39.8
SFT	P+C	750M	46.4	21.9	49.6	37.0	29.5	25.4	24.4	27.9	0.6	27.5	56.4	48.0	51.5	32.4	65.6	18.6	41.6
KD	P+C	250M	49.2	33.5	60.8	46.8	36.2	38.6	24.6	17.2	17.1	41.6	57.0	45.3	55.4	32.4	64.4	32.0	40.9
KD	P+C	500M	50.2	33.6	61.5	46.2	35.9	37.0	30.4	17.6	15.8	46.9	56.3	45.2	54.5	31.7	64.4	30.0	42.4
KD	P+C	750M	49.2	33.0	60.4	47.3	37.7	37.5	33.7	10.5	20.1	42.3	56.4	45.3	54.0	32.6	64.5	28.9	41.6
SFT	C	250M	48.6	26.8	55.1	41.5	29.3	32.5	19.3	28.9	1.8	27.4	55.7	45.7	55.1	30.8	64.6	40.5	34.8
SFT	C	500M	49.1	23.7	52.6	38.6	27.1	33.7	14.2	32.9	1.2	29.8	55.2	46.1	54.6	31.6	64.9	43.5	34.1
SFT	C	750M	46.7	24.2	51.9	38.5	27.6	31.8	18.2	29.9	0.0	31.2	55.3	46.1	54.3	30.2	65.6	37.5	30.3
KD	C	250M	48.9	35.4	65.6	48.8	37.9	41.6	36.2	35.8	18.3	44.7	56.4	44.9	54.9	31.7	65.2	40.6	37.7
KD	C	500M	48.1	33.9	64.1	50.0	39.9	40.7	38.2	39.8	21.9	47.5	55.8	45.0	54.8	31.1	65.1	36.5	39.2
KD	C	750M	49.4	32.3	62.3	47.0	41.0	39.0	39.2	37.9	25.0	49.0	56.3	45.0	54.9	32.3	65.0	37.1	39.1

this choice. The trade-off is that language modeling ability improves more slowly, since the loss is applied to fewer tokens.

Training Duration. Under KD with completion-only masking, average generation performance is roughly stable across token budgets, but individual benchmarks vary substantially. Chinese knowledge benchmarks (C-Eval, CMMLU), instruction following (IFEval), and code generation (HumanEval) improve monotonically, while HellaSwag, ARC-E, and MMLU-Redux decline (Table 5). One plausible explanation is the language composition of the training data: both the pretraining dataset used and the teacher-aligned instruction data are Chinese-heavy, which may preferentially reinforce Chinese-language capabilities at the expense of English benchmarks. Merging Stages 3a and 3b into a single phase with interleaved pretraining and instruction data circumvents this differential pattern and scales more gracefully, but underperforms the sequential pipeline at matched compute budgets (Appendix H).

Evaluation Metric Discrepancy. The differences above are primarily visible under generation-based evaluation. Perplexity-based evaluation (Table 5, right) often compresses differences and can even invert the relative ranking of KD and SFT on the same benchmark (e.g. HellaSwag). These discrepancies underscore that perplexity is an unreliable proxy for generation quality in distilled hybrid models.

6.5 Freezing attention layers

Table 6: Effect of freezing attention layers during Stage 3b. Generation-based evaluation (left) reveals large improvements from freezing ($\bar{\Delta}$ =5.2pp), while perplexity-based evaluation (right) shows negligible differences ($\bar{\Delta}$ =0.4pp). Best result per column in **bold**.

Frozen?	Generation-based (EvalScope)						Perplexity-based (LM-Eval)					
	WG	HS	ARC-E	ARC-C	C-Eval	MMLU-R	WG	HS	ARC-E	ARC-C	CMMLU	MMLU
No	40.7	17.5	50.0	37.7	35.7	35.8	50.6	39.9	42.2	29.4	35.9	29.7
Yes	47.5	23.7	57.8	43.5	37.3	39.0	51.2	40.0	43.4	30.0	36.7	29.5

A natural question is how to preserve the quality of the retained attention layers during instruction tuning. Table 6 compares frozen versus unfrozen attention layers during Stage 3b under both evaluation protocols. Freezing attention weights significantly improves generation-based performance across every benchmark. Unfrozen attention layers allow the instruction-tuning loss to overwrite pretrained representations, causing catastrophic forgetting of the reasoning capabilities acquired during pretraining. Critically, perplexity-based evaluation almost entirely masks this effect. The same frozen/unfrozen comparison that produces 5–8pp generation improvements yields less than 1pp differences on perplexity metrics (Δ -row, Table 6, right). We further investigate whether MLP parameters exhibit the same sensitivity in Appendix G.

7 Discussion

Across every major ablation — objective, masking, training duration (Table 5), freezing (Table 6), and architecture (Section 6.1) — perplexity and generation accuracy tell different stories. Perplexity compresses differences and can even invert rankings (e.g. SFT achieves lower perplexity than KD despite 8–11 pp worse generation accuracy). This pattern extends beyond 0.6B: Table 1 shows a 0.2 pp vs. 20.8 pp teacher–student gap at 7B scale under the two protocols. We therefore argue that generation-based evaluation should be the primary protocol for distilled models.

Under this lens, our ablations identify three critical design choices: (i) KD with completion-only masking, (ii) teacher-aligned instruction data, and (iii) frozen attention layers during Stage 3b. These choices work together because they all preserve teacher structure while concentrating the student’s limited capacity on the most informative signal — soft targets on completions from a teacher-aligned distribution. KD provides richer supervision than one-hot labels, completion-only masking focuses that supervision on answer tokens, teacher-aligned data ensures distributional match, and frozen attention layers prevent catastrophic forgetting of pretrained representations. Pretraining distillation (Stage 3a) monotonically improves KL alignment but has diminishing returns on generation quality (Table 3), suggesting that compute is better spent on Stage 3b once a basic distributional foundation is established.

Extending Stage 3b does not uniformly improve all benchmarks: Chinese knowledge and instruction following improve while some English benchmarks decline, likely due to language composition of the training data. Merging Stages 3a and 3b into a single phase underperforms the sequential pipeline at matched compute (Appendix H). Among architectures, Hybrid KDA consistently outperforms Mamba2 alternatives, with the advantage most visible on hard reasoning tasks; efficiency gains are context-length-dependent, becoming decisive at 32K+ tokens (Figure 2).

7.1 Limitations

All systematic ablations are conducted at 0.6B parameters. While the evaluation gap between perplexity and generation quality should generalize across scales (Table 1 corroborates this at 7B), the specific recipe recommendations may require re-tuning at larger model sizes, and publicly available baselines (e.g. Llama-8B, QRWKV6-7B) operate at different scales, precluding a controlled comparison. Our architecture comparison is also limited to KDA and Mamba2; other expressive linear mixers (e.g. Gated DeltaNet, RWKV-7) were not evaluated. Long-context quality remains an open gap: distillation on 4K-token sequences does not transfer, with Hybrid KDA retaining only 58% of teacher accuracy on LongBench (Appendix L). Targeted long-context training stages (Chen et al., 2026), on-policy distillation (Agarwal et al., 2024), and dataset composition strategies (curriculum ordering, mixing ratios) are promising directions for closing the remaining gaps.

8 Conclusion

This work shows that producing distilled hybrid models with genuine generation quality requires jointly designing the student architecture and the distillation pipeline, guided by generation-based evaluation. Perplexity-based metrics, still the norm in cross-architecture distillation, are a systematically misleading proxy: the divergence appeared consistently across every design axis in our 0.6B-parameter ablations and is corroborated at 7B scale (Table 1). While the general limitation of perplexity is well-known, our results show this gap is especially severe in cross-architecture distillation, where perplexity-only reporting can lead to incorrect conclusions about which methods actually produce models that generate well. We argue that generation-based evaluation should be the primary protocol in this setting.

On the practical side, GenDistill’s systematic ablations yield a concrete distillation recipe: KD with completion-only masking, teacher-aligned instruction data, and frozen attention layers. This combination produces a Hybrid-KDA student that retains 86–90% of teacher accuracy on knowledge benchmarks while reducing KV cache memory by $\sim 75\%$. The key open question is whether these specific recipe recommendations, not just the evaluation gap, hold at larger scales where models have greater capacity and training

dynamics may shift. Validating the recipe at 1B–7B parameters, and extending it with dedicated long-context training, are the most pressing directions for future work.

References

- Rishabh Agarwal, Nino Vieillard, Yongchao Zhou, Piotr Stanczyk, Sabela Ramos, Matthieu Geist, and Olivier Bachem. On-policy distillation of language models: Learning from self-generated mistakes. In *International Conference on Learning Representations (ICLR)*, 2024.
- Yushi Bai, Xin Lv, Jiajie Zhang, Hongchang Lyu, Jiankai Tang, Zhidian Huang, Zhengxiao Du, Xiao Liu, Aohan Zeng, Lei Hou, Yuxiao Dong, Jie Tang, and Juanzi Li. Longbench: A bilingual, multitask benchmark for long context understanding. In *Proceedings of the 62nd Annual Meeting of the Association for Computational Linguistics (Volume 1: Long Papers)*, pp. 3119–3137, 2024.
- Elie Bakouch, Loubna Ben Allal, Anton Lozhkov, Nouamane Tazi, Lewis Tunstall, Carlos Miguel Patiño, Edward Beeching, Aymeric Roucher, Aksel Joonas Reedi, Quentin Gallouédec, Kashif Rasul, Nathan Habib, Clémentine Fourrier, Hynek Kydlicek, Guilherme Penedo, Hugo Larcher, Mathieu Morlon, Vaibhav Srivastav, Joshua Lochner, Xuan-Son Nguyen, Colin Raffel, Leandro von Werra, and Thomas Wolf. SmoLM3: smol, multilingual, long-context reasoner. <https://huggingface.co/blog/smolm3>, 2025.
- Aviv Bick, Kevin Li, Eric Xing, J Zico Kolter, and Albert Gu. Transformers to ssms: Distilling quadratic knowledge to subquadratic models. *Advances in Neural Information Processing Systems*, 37:31788–31812, 2024.
- Aviv Bick, Tobias Katsch, Nimit Sohoni, Arjun Desai, and Albert Gu. Llama: Scaling distilled recurrent models for efficient language processing. In *The Thirteenth International Conference on Learning Representations (ICLR)*, 2025a.
- Aviv Bick, Eric Xing, and Albert Gu. Understanding the skill gap in recurrent language models: The role of the gather-and-aggregate mechanism. In *Proceedings of the 42nd International Conference on Machine Learning*, volume 267, pp. 4324–4344. PMLR, 2025b.
- Yonatan Bisk, Rowan Zellers, Ronan Le Bras, Jianfeng Gao, and Yejin Choi. Piqa: Reasoning about physical commonsense in natural language. In *Proceedings of the AAAI Conference on Artificial Intelligence*, volume 34, pp. 7432–7439, 2020.
- Hanting Chen, Zhicheng Liu, Xutao Wang, Yuchuan Tian, and Yunhe Wang. Dijiang: Efficient large language models through compact kernelization. In *Proceedings of the 41st International Conference on Machine Learning*, volume 235. PMLR, 2024.
- Mark Chen, Jerry Tworek, Heewoo Jun, Qiming Yuan, Henrique Ponde de Oliveira Pinto, Jared Kaplan, Harri Edwards, Yuri Burda, Nicholas Joseph, Greg Brockman, et al. Evaluating large language models trained on code, 2021.
- Yingfa Chen, Zhen Leng Thai, Zihan Zhou, Zhu Zhang, Xingyu Shen, Shuo Wang, Chaojun Xiao, Xu Han, and Zhiyuan Liu. Hybrid linear attention done right: Efficient distillation and effective architectures for extremely long contexts, 2026. URL <https://arxiv.org/abs/2601.22156>.
- Peter Clark, Isaac Cowhey, Oren Etzioni, Tushar Khot, Ashish Sabharwal, Carissa Schoenick, and Oyvind Tafjord. Think you have solved question answering? try arc, the ai2 reasoning challenge, 2018.
- Karl Cobbe, Vineet Kosaraju, Mohammad Bavarian, Mark Chen, Heewoo Jun, Lukasz Kaiser, Matthias Plappert, Jerry Tworek, Jacob Hilton, Reiichiro Nakano, Christopher Hesse, and John Schulman. Training verifiers to solve math word problems, 2021.
- Tri Dao and Albert Gu. Transformers are ssms: Generalized models and efficient algorithms through structured state space duality. In *Proceedings of the 41st International Conference on Machine Learning*, volume 235, pp. 10041–10071. PMLR, 2024.
- Soham De, Samuel L. Smith, Anushan Fernando, Aleksandar Botev, George Cristian-Muraru, Albert Gu, Ruba Haroun, Leonard Berrada, Yutian Chen, Srivatsan Srinivasan, Guillaume Desjardins, Arnaud Doucet, David Budden, Yee Whye Teh, Razvan Pascanu, Nando De Freitas, and Caglar Gulcehre.

-
- Griffin: Mixing gated linear recurrences with local attention for efficient language models, 2024. URL <https://arxiv.org/abs/2402.19427>.
- Xin Dong, Yonggan Fu, Shizhe Diao, Wonmin Byeon, Zijia Chen, Ameya Sunil Mahabaleshwarkar, Shih-Yang Liu, Matthijs Van Keirsbilck, Min-Hung Chen, Yoshi Suhara, Yingyan Lin, Jan Kautz, and Pavlo Molchanov. Hymba: A hybrid-head architecture for small language models. In *International Conference on Learning Representations (ICLR)*, 2025.
- Leo Gao, Jonathan Tow, Baber Abbasi, Stella Biderman, Sid Black, Anthony DiPofi, Charles Foster, Laurence Golber, Jeffrey Hsu, Alain Le Noac’h, Haonan Li, Kyle McDonell, Niklas Muennighoff, Chris Ociepa, Jason Phang, Laria Reynolds, Hailey Schoelkopf, Aviya Skowron, Lintang Sutawika, Eric Tang, Anish Thite, Ben Wang, Kevin Wang, and Andy Zou. A framework for few-shot language model evaluation, 2024. URL <https://zenodo.org/records/10256836>.
- Aryo Pradipta Gema, Joshua Ong Jun Leang, Giwon Hong, Alessio Devoto, Alberto Carlo Maria Mancino, Rohit Saxena, Xuanli He, Yu Zhao, Xiaotang Du, Mohammad Reza Ghasemi Madani, Claire Gardent, Minghao Wu, Alham Fikri Aji, Harish Tayyar Madabushi, and Pasquale Minervini. Are we done with mmlu? In *Proceedings of the 2025 Conference of the Nations of the Americas Chapter of the Association for Computational Linguistics (NAACL)*, pp. 5069–5096, 2025.
- Daniel Goldstein, Eric Alcaide, Janna Lu, and Eugene Cheah. Radlads: Rapid attention distillation to linear attention decoders at scale. In *Conference on Language Modeling (COLM)*, 2025.
- Albert Gu and Tri Dao. Mamba: Linear-time sequence modeling with selective state spaces. In *First Conference on Language Modeling (COLM)*, 2024.
- Yuxian Gu, Qinghao Hu, Shang Yang, Haocheng Xi, Junyu Chen, Song Han, and Han Cai. Jet-nemotron: Efficient language model with post neural architecture search, 2025. URL <https://arxiv.org/abs/2508.15884>.
- Cheng-Ping Hsieh, Simeng Sun, Samuel Kriman, Shantanu Acharya, Dima Rekesh, Fei Jia, Yang Zhang, and Boris Ginsburg. Ruler: What’s the real context size of your long-context language models? In *Proceedings of the 1st Conference on Language Modeling (COLM)*, 2024.
- Yuzhen Huang, Yuzhuo Bai, Zhihao Zhu, Junlei Zhang, Jinghan Zhang, Tangjun Su, Junteng Liu, Chuancheng Lv, Yikai Zhang, Jiayi Lei, Yao Fu, Maosong Sun, and Junxian He. C-eval: A multi-level multi-discipline chinese evaluation suite for foundation models. *Advances in Neural Information Processing Systems*, 36, 2023.
- Angelos Katharopoulos, Apoorv Vyas, Nikolaos Pappas, and François Fleuret. Transformers are RNNs: Fast autoregressive transformers with linear attention. In *International Conference on Machine Learning*, pp. 5156–5165. PMLR, 2020.
- Juan Gabriel Kostelec and Qinghai Guo. Flasheva: Accelerating llm inference via efficient attention, 2025. URL <https://arxiv.org/abs/2511.00576>.
- Haonan Li, Yixuan Zhang, Fajri Koto, Yifei Yang, Hai Zhao, Yeyun Gong, Nan Duan, and Timothy Baldwin. CMMLU: Measuring massive multitask language understanding in Chinese. In *Findings of the Association for Computational Linguistics: ACL 2024*, pp. 11260–11285, 2024.
- Yanhong Li, Songlin Yang, Shawn Tan, Mayank Mishra, Rameswar Panda, Jiawei Zhou, and Yoon Kim. Distilling to hybrid attention models via kl-guided layer selection. In *Proceedings of the Fourteenth International Conference on Learning Representations (ICLR)*, 2026.
- Opher Lieber, Barak Lenz, Hofit Bata, Gal Cohen, Jhonathan Osin, Itay Dalmedigos, Erez Safahi, Shaked Meirom, Yonatan Belinkov, Shai Shalev-Shwartz, Omri Abend, Raz Alon, Tomer Asida, Amir Bergman, Roman Glozman, Michael Gokhman, Avshalom Manevich, Nir Ratner, Noam Rozen, Erez Shwartz, Mor Zusman, and Yoav Shoham. Jamba: A hybrid transformer-mamba language model. In *The Thirteenth International Conference on Learning Representations (ICLR)*, 2025.

-
- Yueyu Lin, Zhiyuan Li, Peter Yue, and Xiao Liu. Arkv: Pretrain is not what we need, an rnn-attention-based language model born from transformer, 2025.
- Jean Mercat, Igor Vasiljevic, Sedrick Keh, Kushal Arora, Achal Dave, Adrien Gaidon, and Thomas Kollar. Linearizing large language models. In *First Conference on Language Modeling (COLM)*, 2024.
- ModelScope Team. Evalscope: A framework for model evaluation, 2024. URL <https://github.com/modelscope/evalscope>.
- Dhruv Nathawani, Igor Gitman, Somshubra Majumdar, Evelina Bakhturina, Ameya Sunil Mahabaleshwar, Jian Zhang, and Jane Polak Scowcroft. Nemotron-Post-Training-Dataset-v1, 07 2025. URL <https://huggingface.co/datasets/nvidia/Nemotron-Post-Training-Dataset-v1>.
- Denis Paperno, Germán Kruszewski, Angeliki Lazaridou, Ngoc Quan Pham, Raffaella Bernardi, Gemma Boleda, Raquel Fernández, and Marco Baroni. The lambada dataset: Word prediction requiring a broad discourse context. In *Proceedings of the 54th Annual Meeting of the Association for Computational Linguistics*, pp. 1525–1534, 2016.
- Bo Peng, Eric Alcaide, Haowen Hou, Guangyu Song, Johan S. Wind, Ruichong Zhang, William Merrill, Daniel Goldstein, Tianyi Wu, Saiteja Utpala, Janna Lu, Kaifeng Tan, Nathan Wilce, Daniel Wuttke, and Christian Zhou-Zheng. Rwkv-7 "goose" with expressive dynamic state evolution, 2025. URL <https://arxiv.org/abs/2503.14456>.
- Keisuke Sakaguchi, Ronan Le Bras, Chandra Bhagavatula, and Yejin Choi. Winogrande: An adversarial winograd schema challenge at scale. *Communications of the ACM*, 64(9):99–106, 2021.
- Imanol Schlag, Kazuki Irie, and Jürgen Schmidhuber. Linear transformers are secretly fast weight programmers. In *International Conference on Machine Learning*, pp. 9355–9366. PMLR, 2021.
- Mirac Suzgun, Nathan Scales, Nathanael Schärli, Sebastian Gehrmann, Yi Tay, Hyung Won Chung, Aakanksha Chowdhery, Quoc V. Le, Ed H. Chi, Denny Zhou, and Jason Wei. Challenging BIG-Bench Tasks and Whether Chain-of-Thought Can Solve Them. In *Findings of the Association for Computational Linguistics: ACL 2023*, pp. 13003–13051, 2023.
- Kimi Team, Yu Zhang, Zongyu Lin, Xingcheng Yao, Jiayi Hu, Fanqing Meng, Chengyin Liu, Xin Men, Songlin Yang, Zhiyuan Li, Wentao Li, Enzhe Lu, Weizhou Liu, Yanru Chen, Weixin Xu, Longhui Yu, Yejie Wang, Yu Fan, Longguang Zhong, Enming Yuan, Dehao Zhang, Yizhi Zhang, T. Y. Liu, Haiming Wang, Shengjun Fang, Weiran He, Shaowei Liu, Yiwei Li, Jianlin Su, Jiezhong Qiu, Bo Pang, Junjie Yan, Zhejun Jiang, Weixiao Huang, Bohong Yin, Jiacheng You, Chu Wei, Zhengtao Wang, Chao Hong, Yutian Chen, Guanduo Chen, Yucheng Wang, Huabin Zheng, Feng Wang, Yibo Liu, Mengnan Dong, Zheng Zhang, Siyuan Pan, Wenhao Wu, Yuhao Wu, Longyu Guan, Jiawen Tao, Guohong Fu, Xinran Xu, Yuzhi Wang, Guokun Lai, Yuxin Wu, Xinyu Zhou, Zhilin Yang, and Yulun Du. Kimi linear: An expressive, efficient attention architecture, 2025. URL <https://arxiv.org/abs/2510.26692>.
- MiniCPM Team, Wenhao An, Yingfa Chen, Yewei Fang, Jiayi Li, Xin Li, Yaohui Li, Yishan Li, Yuxuan Li, Biyuan Lin, Chuan Liu, Hezi Liu, Siyuan Liu, Hongya Lyu, Yinxu Pan, Shixin Ren, Xingyu Shen, Zhou Su, Haojun Sun, Yangang Sun, Zhen Leng Thai, Xin Tian, Rui Wang, Xiaorong Wang, Yudong Wang, Bo Wu, Xiaoyue Xu, Dong Xu, Shuaikang Xue, Jiawei Yang, Bowen Zhang, Jinqian Zhang, Letian Zhang, Shengnan Zhang, Xinyu Zhang, Xinyuan Zhang, Zhu Zhang, Hengyu Zhao, Jiacheng Zhao, Jie Zhou, Zihan Zhou, Shuo Wang, Chaojun Xiao, Xu Han, Zhiyuan Liu, and Maosong Sun. Minicpm-sala: Hybridizing sparse and linear attention for efficient long-context modeling, 2026. URL <https://arxiv.org/abs/2602.11761>.
- Teknium. Openhermes 2.5: An open dataset of synthetic data for generalist llm assistants, 2023. URL <https://huggingface.co/datasets/teknium/OpenHermes-2.5>.
- Xiaoyu Tian, Yunjie Ji, Haotian Wang, Shuaiting Chen, Sitong Zhao, Yiping Peng, Han Zhao, and Xiangang Li. Not all correct answers are equal: Why your distillation source matters, 2025. URL <https://arxiv.org/abs/2505.14464>.

-
- Junxiong Wang, Daniele Paliotta, Avner May, Alexander M. Rush, and Tri Dao. The mamba in the llama: Distilling and accelerating hybrid models. In *Advances in Neural Information Processing Systems 37 (NeurIPS)*, 2024.
- Junxiong Wang, Wen-Ding Li, Daniele Paliotta, Daniel Ritter, Alexander M. Rush, and Tri Dao. M1: Towards scalable test-time compute with mamba reasoning models, 2025. URL <https://arxiv.org/abs/2504.10449>.
- An Yang, Anfeng Li, Baosong Yang, Beichen Zhang, Binyuan Hui, Bo Zheng, Bowen Yu, Chang Gao, Chengen Huang, Chenxu Lv, Chujie Zheng, Dayiheng Liu, Fan Zhou, Fei Huang, Feng Hu, Hao Ge, Haoran Wei, Huan Lin, Jialong Tang, Jian Yang, Jianhong Tu, Jianwei Zhang, Jianxin Yang, Jiayi Yang, Jing Zhou, Jingren Zhou, Junyang Lin, Kai Dang, Keqin Bao, Kexin Yang, Le Yu, Lianghao Deng, Mei Li, Mingfeng Xue, Mingze Li, Pei Zhang, Peng Wang, Qin Zhu, Rui Men, Ruize Gao, Shixuan Liu, Shuang Luo, Tianhao Li, Tianyi Tang, Wenbiao Yin, Xingzhang Ren, Xinyu Wang, Xinyu Zhang, Xuancheng Ren, Yang Fan, Yang Su, Yichang Zhang, Yinger Zhang, Yu Wan, Yuqiong Liu, Zekun Wang, Zeyu Cui, Zhenru Zhang, Zhipeng Zhou, and Zihan Qiu. Qwen3 technical report, 2025a. URL <https://arxiv.org/abs/2505.09388>.
- Mingyu Yang, Mehdi Rezagholizadeh, Guihong Li, Vikram Appia, and Emad Barsoum. Zebra-llama: Towards extremely efficient hybrid models. In *Advances in Neural Information Processing Systems 38 (NeurIPS)*, 2025b.
- Songlin Yang and Yu Zhang. Fla: A triton-based library for hardware-efficient implementations of linear attention mechanism, January 2024. URL <https://github.com/fla-org/flash-linear-attention>.
- Songlin Yang, Bailin Wang, Yikang Shen, Rameswar Panda, and Yoon Kim. Gated linear attention transformers with hardware-efficient training. In *Proceedings of the 41st International Conference on Machine Learning*, volume 235, pp. 56501–56523. PMLR, 2024a.
- Songlin Yang, Bailin Wang, Yu Zhang, Yikang Shen, and Yoon Kim. Parallelizing linear transformers with the delta rule over sequence length. In *Advances in Neural Information Processing Systems 37 (NeurIPS)*, 2024b.
- Songlin Yang, Jan Kautz, and Ali Hatamizadeh. Gated delta networks: Improving mamba2 with delta rule. In *The Thirteenth International Conference on Learning Representations (ICLR)*, 2025c.
- Rowan Zellers, Ari Holtzman, Yonatan Bisk, Ali Farhadi, and Yejin Choi. Hellaswag: Can a machine really finish your sentence? In *Proceedings of the 57th Annual Meeting of the Association for Computational Linguistics*, 2019.
- Max Zhang. Max’s awesome datasets. <https://github.com/Mxoder/Maxs-Awesome-Datasets>, 2025.
- Michael Zhang, Kush Bhatia, Hermann Kumbong, and Christopher Ré. The hedgehog & the porcupine: Expressive linear attentions with softmax mimicry. In *International Conference on Learning Representations (ICLR)*, 2024.
- Michael Zhang, Simran Arora, Rahul Chalamala, Alan Wu, Benjamin Spector, Aaryan Singhal, Krithik Ramesh, and Christopher Ré. Lolcats: On low-rank linearizing of large language models. In *International Conference on Learning Representations (ICLR)*, 2025.
- Jeffrey Zhou, Tianjian Lu, Swaroop Mishra, Siddhartha Brahma, Sujoy Basu, Yi Luan, Denny Zhou, and Le Hou. Instruction-following evaluation for large language models, 2023.
- Jingwei Zuo, Maksim Velikanov, Ilyas Chahed, Younes Belkada, Dhia Eddine Rhayem, Guillaume Kunsch, Hakim Hacid, Hamza Yous, Brahim Farhat, Ibrahim Khadraoui, Mugariya Farooq, Giulia Campesan, Ruxandra Cojocaru, Yasser Djilali, Shi Hu, Iheb Chaabane, Puneesh Khanna, Mohamed El Amine Seddik, Ngoc Dung Huynh, Phuc Le Khac, Leen AlQadi, Billel Mokeddem, Mohamed Chami, Abdalgader Abubaker, Mikhail Lubinets, Kacper Piskorski, and Slim Frikha. Falcon-h1: A family of hybrid-head language models redefining efficiency and performance, 2025. URL <https://arxiv.org/abs/2507.22448>.

This appendix provides supplementary details and ablation studies:

- Appendix A: Model Architecture Details
- Appendix B: Hyperparameter Details
- Appendix C: Architecture Design Choices
- Appendix D: Attention Layer Selection Ablation
- Appendix E: Top-K Sparsification and CE Loss Weight
- Appendix F: Learning Rate Ablation
- Appendix G: Frozen MLP Ablation
- Appendix H: Combined Stage Mixing
- Appendix I: Extended Stage 3b Results
- Appendix J: Perplexity-Based Architecture Comparison
- Appendix K: Maximum Throughput Under GPU Saturation
- Appendix L: Long-Context Quality

A Model Architecture Details

Base model (teacher). We distill from Qwen3-0.6B, a dense Transformer with grouped-query attention. Table 7 summarizes its configuration.

Table 7: Qwen3-0.6B base model (teacher) configuration.

Parameter	Value
Hidden dimension (d_{model})	1024
Number of layers	28
Attention heads (Q)	16
KV heads (GQA)	8
Head dimension	128
Intermediate size (MLP)	3072
Vocabulary size	151,936
Max position embeddings	40,960
RoPE θ	1,000,000
RMSNorm ϵ	1e-6
MLP activation	SiLU
Tie word embeddings	Yes

The student models are based on the 596M-parameter teacher (non-embedding) but replace a subset of attention layers with alternative sequence mixers. Each mixer layer introduces additional gating, convolution, and state-management parameters beyond the original Q/K/V/O projections, increasing the total parameter count: KDA adds $\sim 0.8\text{M}$ per replaced layer (short convolutions on Q/K/V, gating projections for the delta rule), while Mamba2 adds $\sim 2.1\text{M}$ per replaced layer (a larger joint input projection that maps to the SSM state components, time-step, and gating dimensions). Table 8 details the mixer configurations. Each mixer layer replaces the self-attention block while retaining the original MLP, layer norms, and residual connections. Pure KDA and Mamba variants use identical mixer configurations but replace all 28 layers.

Table 8: Hybrid student mixer configurations (Qwen3-0.6B scale). KDA = Kimi Delta Attention.

Parameter	KDA	Mamba2
Retained attention layers	7 of 28	7 of 28
Attn. layer indices	{0,2,6,11,13,18,21}	{0,2,6,11,13,18,21}
State dimension (d_{state})	128 per head	128 per head
Q heads	16	16
K/V heads (GQA)	8	8
Head dimension (Q/K/V)	128 / 128 / 128	128 / 128 / 128
Chunk size	128	128
Short convolution kernel	4	4
Output gate activation	SiLU	SiLU
Post-SSM normalization	No	No
QK normalization (RMSNORM)	Yes	No
Initialization	VO ^a	VO ^a
Non-embedding parameters	613M	641M

^aTeacher’s V and O projection weights used to initialize the corresponding mixer parameters.

B Hyperparameter Details

Table 9 lists the full hyperparameter configuration for each distillation stage. Stage 1 aligns the outputs of the attention layer between the two models, while Stage 2 aligns the outputs of the whole attention block via L2 loss on pretraining data. The Stage 1 only trains the Q and K projections, keeping the conv1d (identity initialized) and other parameters fixed. Stage 2, meanwhile, trains all mixer parameters. Stages 3a and 3b perform end-to-end knowledge distillation with forward KL divergence. Both stages freeze the attention layers to prevent catastrophic forgetting of the representations inherited from the teacher model. Stage 3b switches to instruction data with completion-only masking (see Section 6.5). All stages use AdamW with $(\beta_1, \beta_2) = (0.9, 0.95)$, a warmup-stable-decay learning rate schedule (10% warmup, 10% decay, minimum LR ratio 0.02), weight decay 0.1, gradient clipping at 1.0, bf16 mixed precision, and DeepSpeed ZeRO Stage 2.

Evaluation configurations. We use two complementary evaluation frameworks, chosen to highlight the PPL-vs-generation gap that is a central finding of this work. All evaluations use a batch size of 64 and the SDPA (Scaled Dot-Product Attention) backend. *EvalScope (generation-based)*: Models are evaluated using the recommended sampling setup: temperature=0.7, top-p=0.8, top-k=20, and seed=42. Maximum new tokens is set to 1024. Few-shot settings: C-Eval (5-shot), MMLU / MMLU-Redux (5-shot), ARC-Easy / ARC-Challenge (0-shot), HellaSwag (0-shot), WinoGrande (0-shot), GSM8K (4-shot chain-of-thought), CMMLU (0-shot), BBH (0-shot), HumanEval (0-shot), IFEval (0-shot), TruthfulQA (0-shot). *LM-Eval Harness (perplexity-based)*: Models are evaluated on likelihood-based scoring. Tasks: ARC-Easy, ARC-Challenge, HellaSwag, WinoGrande, PIQA, LAMBADA (OpenAI), MMLU. We use 3 seeds for the evals, seeds = 1, 2, 3.

C Architecture Design Choices

We conduct an ablation study to analyze the impact of key architectural choices on the distilled hybrid model. Specifically, we investigate: (i) the output gate activation function (SiLU vs. Sigmoid), (ii) the presence of a post-SSM normalization layer, and (iii) the initialization strategy for the mixer parameters (VO initialization from the teacher’s value and output projections, QKVO initialization from all attention projections, or random initialization). For each configuration, we run the three-stage distillation pipeline on the FineWeb-Edu dataset (for stage 3 we do not train on the instruct data, but only the 100M tokens on the FineWeb-Edu) and report the evaluation perplexity at the end of training.

We find Stage 1 to be critical for stable and strong distillation: skipping Stage 1 significantly degrades performance, even when initializing from the teacher, while fully random initialization remains competitive but worse overall, consistent with observations in prior attention-to-linear distillation work (Goldstein et al.,

Table 9: Hyperparameters for each distillation stage.

Hyperparameter	Stage 1 <i>(Mixer alignment)</i>	Stage 2 <i>(Hidden-state align.)</i>	Stage 3a <i>(End-to-end KD)</i>	Stage 3b <i>(Instruction KD)</i>
<i>Data</i>				
Dataset	FineWeb-EDU + FW-EDU-Chinese	FineWeb-EDU + FW-EDU-Chinese	FineWeb-EDU + FW-EDU-Chinese	AM-Qwen3-Distilled (completion-only, packed)
Tokens	30M	30M	500M	500M
Sequence length	2048	2048	2048	4096
<i>Optimization</i>				
Learning rate	5e-4	1e-4	2.5e-5	2.5e-5
Per-device batch size	8	8	2	2
Gradient accumulation	1	1	16	16
Effective batch size (2 GPUs)	16	16	64	64
<i>Loss</i>				
Training objective	L2 norm (mixer layer output align.)	L2 norm (attention block output align.)	Forward KL divergence	Forward KL divergence
KD temperature τ	—	—	1.0	1.0
CE loss weight α_{CE}	—	—	0.0	0.0
Top- K	—	—	None (full vocab)	None (full vocab)
<i>Parameter Freezing</i>				
Frozen parameters	None	None	Attention layers	Attention layers
MLP active	No	Yes	Yes	Yes

Table 10: Ablation study on model architecture details. We report evaluation perplexity on FineWeb-Edu after completing Stages 1–3 of distillation.

Configuration	Gate	Post-SSM Norm	Initialization	Eval PPL ↓
Baseline (Ours)	SiLU	✗	VO	21.32
Sigmoid gate	Sigmoid	✗	VO	21.64
Post-SSM norm	SiLU	✓	VO	21.47
QKVO init	SiLU	✗	QKVO	21.25
QKVO init (no Stage 1)	SiLU	✗	QKVO	25.41
VO init (no Stage 1)	SiLU	✗	VO	24.42
Random init	SiLU	✗	Random	24.88

2025). Using a Sigmoid gate underperforms SiLU. We hypothesize this is partly because Sigmoid does not admit an identity-style initialization for the gate during distillation, which may hinder optimization. Adding a post-SSM normalization layer is slightly worse in perplexity and, in our downstream evaluation, shows a larger drop and we therefore omit it (and we also observed it to be substantially worse in our Mamba-based hybrids). Finally, QKVO initialization performs similarly (slightly better for the KDA models) than VO-only initialization, however, in early Mamba-based experiments the gap was larger in the opposite direction, so we default to VO initialization for a fairer comparison across architectures.

D Attention Layer Selection Ablation

We compare beam search layer selection against three baselines for the attention budget of 5 attention layers. We choose this, as with increasing number of attention layers the performance will converge to the teacher model’s performance and the gap between methods will therefore be smaller. We compare the following selection methods:

- **Uniform:** Layers are spaced at equal intervals.
- **Greedy:** Selects top- k layers by individual perplexity impact.
- **Greedy Aggregate (Learned):** Starts from a linear model and adds attention layers based on held-out KL divergence after training the resulting hybrid models (Li et al., 2026).

- **Beam Search Add:** Starts from a full KDA model and adds attention layers to maximize performance.
- **Beam Search Replace:** starts with a full transformer and progressively replaces attention layers with KDA layers, minimizing perplexity degradation.

Evaluation Tasks. We consider evaluating the layer importance on three tasks, and use the average performance on all 3 tasks as the importance measure:

- **AR (Associative Recall):** A synthetic key-value retrieval task that directly tests in-context retrieval capabilities. We use 40 key-value pairs per example with 500 total examples.
- **CEVAL:** Chinese language understanding benchmark (similar task to MMLU, whose performance has been shown to be highly influenced by the choice of attention layers (Bick et al., 2025b)).
- **Fineweb-EDU:** General language modeling perplexity on educational web text.

Table 11 lists selected indices. Table 12 reports downstream performance. Greedy Aggregate achieves the lowest evaluation loss (Figure 4) but underperforms on downstream tasks. Beam Add achieves the best balance of reasoning and knowledge (Table 12), outperforming both Beam Replace and Greedy Learned. We therefore use the attention layers selected by the Beam Search Add method in all our remaining experiments.

Table 11: Attention layer selection for different methods and sparsity levels (Qwen3-0.6B, 28 layers). Layer indices are 0-indexed.

Method	5 Attn Layers	7 Attn Layers	9 Attn Layers
Uniform	{0,6,11,16,21}	{0,5,9,13,17,21,25}	{0,3,6,9,12,15,18,21,24}
Learned Selection (Greedy Aggregate, KL)	{6,16,19,20,21}	{6,8,11,16,19,20,21}	{2,6,8,11,16,18,19,20,21}
Greedy	{0,2,11,13,18}	{0,2,5,11,13,16,18}	{0,1,2,5,7,11,13,16,18}
Beam Search Add	{2,11,12,17,21}	{0,2,6,11,13,18,21}	{0,1,2,6,11,17,18,19,21}
Beam Search Replace	{0,3,12,14,23}	{0,3,12,14,18,23,24}	{0,3,7,12,14,18,23,24,25}

Table 12: Downstream performance after Stage 3b for the selected attention-layer configurations.

Config (Stage 3b)	CEVAL \uparrow	ARC-C \uparrow	ARC-E \uparrow	WG \uparrow	HS \uparrow	PIQA \uparrow	MMLU-redux \uparrow
Uniform	35.1	42.8	56.1	44.5	21.2	64.0	36.1
Greedy Learned	30.3	44.9	60.1	49.5	33.5	64.6	38.7
Beam Replace	26.8	37.3	49.2	51.2	26.6	63.1	32.0
Beam Add	36.0	47.0	59.2	50.2	33.1	64.1	37.1
Greedy	32.3	20.9	30.3	31.4	12.3	64.2	27.3

E Top-K Sparsification and CE Loss Weight

We ablate top- K sparsification of the KD target distribution and the cross-entropy loss weight α_{CE} . Ta-

Table 13: Effect of top- K sparsification of the KD loss during Stage 3b with frozen attention. All runs use 7 attention layers, `freeze_attn=True`, KD with completion-only masking, and 250M tokens. Generation-based evaluation (EvalScope). Best result per column in **bold**.

Top- K	C-Eval	MMLU-R	CMMLU	ARC-E	ARC-C	HS	WG	BBH	GSM8K	HEval	IFEval	Avg.
None (baseline)	39.4	39.3	37.7	63.0	50.9	36.4	49.6	19.2	35.7	17.1	45.5	39.4
$K = 100$	34.9	38.3	38.0	63.8	50.9	35.6	49.6	18.3	35.1	20.1	43.8	38.9
$K = 500$	35.9	39.0	37.0	63.1	49.5	36.4	48.8	18.8	32.6	18.3	44.4	38.5
$K = 1,000$	34.9	38.8	37.7	63.9	50.3	36.5	50.4	18.4	33.6	19.5	44.9	39.0
$K = 10,000$	35.8	38.7	38.1	63.7	49.9	36.1	51.1	18.1	32.4	20.7	45.3	39.1

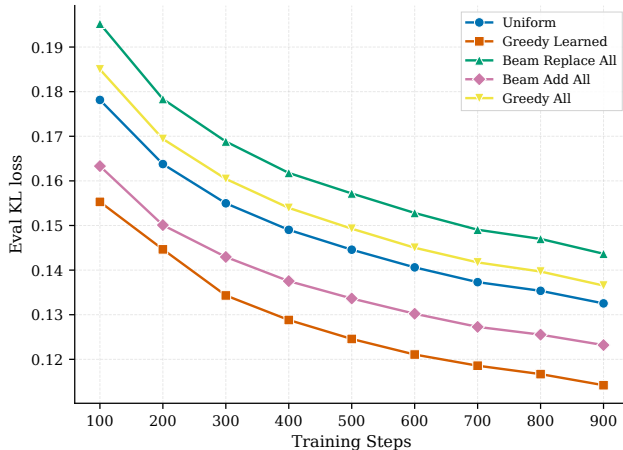


Figure 4: Evaluation loss curves for attention layer selection methods during Stage 3b. Greedy Learned achieves the lowest loss but Beam Add yields better downstream performance.

ble 13 shows that restricting the KD loss to the teacher’s top- K tokens does not improve performance when attention layers are frozen. The full-vocabulary baseline achieves the highest average score across all eleven benchmarks, with the largest advantages on knowledge-intensive tasks (C-Eval, MMLU-Redux, GSM8K). Commonsense benchmarks show no systematic trend across K values. We therefore use full-vocabulary KD for all main experiments. Adding any cross-entropy weight substantially degrades knowledge benchmarks

Table 14: Effect of cross-entropy loss weight α_{CE} in the KD objective ($\mathcal{L} = \mathcal{L}_{KL} + \alpha_{CE}\mathcal{L}_{CE}$). All runs use 5 attention layers, `freeze_attn=False`, 500M tokens.

α_{CE}	WG	HS	ARC-E	ARC-C	C-Eval	MMLU-R
Default	40.7	17.5	50.0	37.7	35.7	35.8
0.1	40.8	18.3	44.0	31.1	22.3	28.3
0.035	44.0	16.7	48.8	36.7	22.9	33.5
0.01	43.4	17.0	51.2	38.2	27.3	34.4

(Table 14): even $\alpha_{CE} = 0.01$ drops C-Eval by 8.4 points and MMLU-R by 1.4 points, while higher values cause catastrophic drops. We accordingly set $\alpha_{CE} = 0.0$ for all main experiments.

F Learning Rate Ablation

Section 6.4 shows that several generation benchmarks (HellaSwag, ARC-E, MMLU-Redux) degrade as Stage 3b training continues at LR=2.5e-5. Here we test whether a smaller learning rate (LR=1e-5) mitigates this effect by slowing the update dynamics, keeping all other settings fixed (KD with completion-only masking) and varying the training token budget. Table 15 shows that a modest learning-rate reduction does not remove the downward trend on several generation metrics with additional Stage 3b tokens: ARC-E and HellaSwag decrease as training continues under both LR settings. In contrast, it slows improvement on knowledge-heavy benchmarks at a fixed token budget: for example, C-Eval at 250M tokens is substantially lower at LR=1e-5 than at LR=2.5e-5. Consequently, we stay with the chosen LR. Note that PPL-based evaluation changes little with learning rate, while differences in generation-based metrics are substantial.

G Frozen MLP Ablation

Section 6.4 shows that several generation benchmarks degrade with extended Stage 3b training and the learning-rate ablation (Appendix F) rules out learning rate as the primary explanation. Here we test whether

Table 15: Learning rate ablation for Stage 3b training with KD loss (KD) and completion-only masking (C). Best student result per column and evaluation method in **bold**.

		Tokens	LR	WG \uparrow	HS \uparrow	ARC-E \uparrow	ARC-C \uparrow	C-Eval \uparrow	MMLU-R \uparrow
Generation	Teacher (Qwen3-0.6B)			51.2	39.0	70.8	55.0	42.9	46.1
	250M	2.5e-5		48.9	35.4	65.6	48.8	37.9	41.6
	500M	2.5e-5		48.1	33.9	64.1	50.0	39.9	40.7
	750M	2.5e-5		49.4	32.3	62.3	47.0	41.0	39.0
	100M	1e-5		49.8	34.0	64.8	49.1	28.8	40.7
	250M	1e-5		48.9	35.5	64.2	47.0	31.3	41.5
	500M	1e-5		48.6	34.7	61.4	48.2	36.9	39.0
				WG \uparrow	HS \uparrow	ARC-E \uparrow	ARC-C \uparrow	PIQA \uparrow	LAMBADA \downarrow
PPL-based	Teacher (Qwen3-0.6B)			55.5	47.3	55.6	34.2	65.9	24.7
	250M	2.5e-5		56.4	44.9	54.9	31.7	65.2	40.6
	500M	2.5e-5		55.8	45.0	54.8	31.1	65.1	36.5
	750M	2.5e-5		56.3	45.0	54.9	32.3	65.0	37.1
	100M	1e-5		57.1	44.8	53.2	31.1	65.4	34.2
	250M	1e-5		55.2	44.9	54.1	31.9	65.5	36.5
	500M	1e-5		55.4	44.9	54.7	31.9	65.7	37.8

the degradation is driven by corruption of factual knowledge stored in MLP parameters by freezing all MLP layers during Stage 3b while keeping all other settings fixed (KD with completion-only masking). Unfrozen KD baselines from Table 5 are reproduced for comparison. Freezing the MLPs does not eliminate the

Table 16: Frozen MLP ablation across training durations. Generation-based (EvalScope, left) and perplexity-based (LM-eval, right) results for Stage 3b with frozen vs. unfrozen MLP parameters under KD with completion-only masking. Unfrozen rows are reproduced from Table 5. HS generation is unavailable for frozen runs⁹. Best student result per column in **bold**.

MLP	Tokens	Generation-based (EvalScope)											Perplexity-based (LM-eval)			
		WG	HS	ARC-E	ARC-C	C-Eval	MMLU-R	CMMMLU	GSM8K	HEval	BBH	IFEval	HS	PIQA	LAM. \downarrow	MMLU
Teacher (Qwen3-0.6B)		51.2	39.0	70.8	55.0	42.9	46.1	45.2	57.5	35.3	27.4	57.1	47.3	65.9	24.7	40.2
Unfrozen	250M	48.9	35.4	65.6	48.8	37.9	41.6	36.2	35.8	18.3	20.5	44.7	44.9	65.2	40.6	37.7
Unfrozen	500M	48.1	33.9	64.1	50.0	39.9	40.7	38.2	39.8	21.9	22.4	47.5	45.0	65.1	36.5	39.2
Unfrozen	750M	49.4	32.3	62.3	47.0	41.0	39.0	39.2	37.9	25.0	22.4	49.0	45.0	65.0	37.1	39.1
Frozen	100M	50.7	-	62.2	47.4	29.9	37.8	32.8	25.1	12.2	15.6	38.6	44.7	67.0	36.9	39.7
Frozen	250M	51.0	-	63.0	47.1	31.4	38.6	31.1	21.8	18.3	16.4	40.8	44.8	66.9	39.4	40.1
Frozen	500M	49.8	-	61.6	45.9	32.1	37.5	27.4	18.7	17.1	16.4	39.9	44.7	66.8	38.8	40.2
Frozen	750M	50.8	-	60.8	45.1	34.5	38.3	24.6	17.2	18.3	15.0	38.5	44.9	66.4	39.4	41.4

degradation on the affected generation benchmarks as Stage 3b training is extended (Table 16). Moreover, the unfrozen baselines generally retain reasoning performance better, suggesting that MLP adaptation is helpful rather than the root cause of the decline. Knowledge-heavy benchmarks exhibit mixed sensitivity to freezing: some remain competitive under frozen MLPs, indicating that mixer and routing updates can absorb part of the distillation signal, while others degrade, consistent with the need for MLP plasticity for broader knowledge transfer (especially cross-lingual). Finally, perplexity-based metrics change little across the duration sweep, again highlighting the gap between PPL-based and generation-based evaluation. These results argue against MLP knowledge corruption as the primary driver of Stage 3b degradation and support keeping MLPs trainable during Stage 3b.

H Combined Stage Mixing

The four-stage sequential pipeline (Section 4.2) trains on pretraining and instruction data in separate stages, which risks Stage 3b overwriting the general language representations acquired during Stage 3a, a pattern visible in the benchmark-specific degradation reported in Section 6.4. We investigate whether merging Stages 3a and 3b into a single training phase with interleaved pretraining and instruction data can circumvent this overwrite pattern while simplifying the pipeline. Table 17 compares the sequential pipeline against

Table 17: Combined stage mixing results. Sequential baselines (top) use the standard pipeline: 500M tokens of Stage 3a pretraining KD followed by Stage 3b instruction KD with completion-only masking and frozen attention. Combined stage runs (bottom) interleave pretraining and instruction data in a single training stage after Stages 1–2. Ratios denote pretrain:instruct data proportions; * indicates balanced FineWeb (50:50 EN:CN rather than the natural 29:71 ratio). Generation-based evaluation (EvalScope). Best student result per column in **bold**.

Configuration	Tokens	C-Eval \uparrow	MMLU-R \uparrow	CMMLU \uparrow	ARC-E \uparrow	ARC-C \uparrow	HS \uparrow	WG \uparrow	GSM8K \uparrow	HEval \uparrow	IFEval \uparrow	LAM. \downarrow
<i>Teacher (Qwen3-0.6B)</i>		42.9	46.1	45.2	70.8	55.0	39.0	51.2	57.5	35.3	57.1	24.7
<i>Sequential pipeline (Stage 3a \rightarrow Stage 3b)</i>												
KD + C, 250M 3b	750M	37.9	41.6	36.2	65.6	48.8	35.4	48.9	35.8	18.3	44.7	40.63
KD + C, 500M 3b	1B	39.9	40.7	38.2	64.1	50.0	33.9	48.1	39.8	21.9	47.5	36.46
KD + C, 750M 3b	1.25B	41.0	39.0	39.2	62.3	47.0	32.3	49.4	37.9	25.0	49.0	37.11
<i>Combined stage mixing (pretrain:instruct ratio)</i>												
50/50	500M	36.0	40.4	28.9	65.2	46.9	34.1	49.2	26.2	17.7	42.9	32.65
67/33	750M	38.1	41.9	31.1	65.2	48.6	31.5	51.8	27.9	17.7	42.1	36.66
50/50	750M	40.1	39.6	34.5	64.9	48.3	29.5	51.0	27.7	17.1	41.4	32.75
50/50*	750M	38.8	39.4	36.9	64.8	49.6	32.7	50.4	29.1	14.6	44.7	33.12
33/67	750M	37.5	39.5	35.4	65.2	49.3	31.8	50.4	30.9	13.4	44.5	34.81
50/50	1B	37.1	41.2	32.8	65.4	49.1	35.3	48.8	28.4	17.7	46.2	32.20
25/75*	1B	39.0	40.8	38.4	65.7	49.7	30.2	49.4	32.2	16.5	45.7	34.52
15/85*	1B	37.5	41.7	38.3	65.3	49.7	31.5	50.8	34.0	15.8	48.2	32.86
10/90*	1B	37.4	40.8	36.6	66.0	49.9	32.8	47.4	35.1	16.5	45.5	34.45
15/85*	2B	38.2	41.2	39.2	67.2	50.0	36.1	50.0	37.1	18.3	48.2	31.13

ten combined-stage configurations varying in total token budget, pretrain-to-instruct ratio, and pretraining data composition. Several patterns emerge. First, at matched compute budgets, the sequential pipeline outperforms combined mixing, with the largest gaps on reasoning and code generation benchmarks; the dedicated pretraining phase in Stage 3a appears to provide a stronger representational foundation than interleaved pretraining can replicate at the same scale. Second, among combined configurations, instruction-heavy ratios consistently outperform pretrain-heavy ones: allocating roughly 85% of tokens to instruction data and retaining only a small pretraining fraction yields the best balance across knowledge, reasoning, and instruction-following tasks. Third, balancing the English-to-Chinese ratio in the pretraining subset (50:50 rather than the natural distribution) consistently improves Chinese knowledge benchmarks without harming English performance, confirming that data composition within the pretraining fraction matters even when that fraction is small. Fourth, unlike the sequential pipeline where extending Stage 3b degrades several benchmarks (Table 5), combined mixing scales gracefully with additional compute, showing steady improvement from medium to large token budgets without the characteristic degradation pattern. Fifth, at sufficient total compute, the best combined configuration approaches or matches the sequential pipeline’s best results across most benchmarks and surpasses it on language modeling and several reasoning tasks, suggesting that combined mixing may become the preferred strategy in higher-compute regimes where the benefits of graceful scaling outweigh the sequential pipeline’s advantage at smaller budgets.

I Extended Stage 3b Results

Table 18 presents the complete results for all Stage 3b configurations across 11 generation-based and 7 perplexity-based benchmarks, complementing the summary in Table 5. KD with completion-only masking achieves the best student result on every generation benchmark. For generation columns, greedy decoding results are shown in parentheses.

Table 18: Extended Stage 3b ablation. Generation-based results (EvalScope, left) with greedy decoding in parentheses; perplexity-based results (LM-eval, right). Best student result per column in **bold**.

Loss	Mask	Tokens	C-Eval	MMLU-R	CMMLU	WG	Generation-based (EvalScope)					Perplexity-based (LM-eval)								
							HS	ARC-E	ARC-C	BBH	GSM8K	HEval	IFEval	WG	HS	ARC-E	ARC-C	PIQA	LAM.↓	MMLU
<i>Teacher</i>			42.9 (43.5)	46.1 (46.0)	45.2 (46.2)	51.2 (51.4)	39.0 (39.3)	70.8 (71.9)	55.0 (56.2)	27.4 (27.4)	57.5 (59.7)	35.3 (33.5)	57.1 (58.2)	55.5	47.3	55.6	34.2	65.9	24.7	40.2
SFT	P+C	250M	32.0 (33.1)	29.3 (34.6)	22.9 (24.3)	46.1 (48.2)	24.1 (28.2)	54.4 (60.5)	39.4 (46.2)	5.1 (5.8)	26.1 (27.9)	2.4 (0.0)	26.2 (24.8)	55.9	47.3	54.4	32.4	65.6	21.2	40.5
SFT	P+C	500M	25.7 (29.0)	28.6 (33.2)	22.5 (23.4)	45.8 (48.6)	23.2 (28.6)	50.1 (59.4)	37.0 (45.1)	8.2 (5.6)	26.5 (26.8)	4.3 (0.0)	26.4 (24.9)	56.0	47.7	52.5	34.0	65.3	20.8	39.8
SFT	P+C	750M	29.5 (33.7)	25.4 (27.3)	24.4 (24.4)	46.4 (48.5)	21.9 (23.1)	49.6 (55.6)	37.0 (40.6)	9.3 (8.8)	27.9 (29.6)	0.6 (0.0)	27.5 (24.4)	56.4	48.0	51.5	32.4	65.6	18.6	41.6
KD	P+C	250M	36.2 (37.4)	38.6 (38.6)	24.6 (22.4)	49.2 (49.9)	33.5 (33.1)	60.8 (61.5)	46.8 (46.7)	17.6 (18.2)	17.2 (20.0)	17.1 (16.5)	41.6 (36.2)	57.0	45.3	55.4	32.4	64.4	32.0	40.9
KD	P+C	500M	35.9 (37.5)	37.0 (38.2)	30.4 (29.8)	50.2 (50.0)	33.6 (33.6)	61.5 (62.1)	46.2 (47.9)	17.5 (18.4)	17.6 (19.6)	15.8 (18.9)	46.9 (39.0)	56.3	45.2	54.5	31.7	64.4	30.0	42.4
KD	P+C	750M	37.7 (39.0)	37.5 (38.7)	33.7 (33.7)	49.2 (49.7)	33.0 (33.0)	60.4 (61.7)	47.3 (47.1)	18.4 (19.4)	10.5 (13.0)	20.1 (20.7)	42.3 (38.1)	56.4	45.3	54.0	32.6	64.5	28.9	41.6
SFT	C	250M	29.3 (28.7)	32.5 (36.0)	19.3 (6.6)	48.6 (49.5)	26.8 (28.7)	55.1 (60.7)	41.5 (46.0)	6.7 (5.3)	28.9 (32.3)	1.8 (0.6)	27.4 (24.0)	55.7	45.7	55.1	30.8	64.6	40.5	34.8
SFT	C	500M	27.1 (29.7)	33.7 (35.2)	14.2 (2.9)	49.1 (49.2)	23.7 (24.4)	52.6 (58.7)	38.6 (42.8)	11.4 (9.3)	32.9 (33.3)	1.2 (1.2)	29.8 (25.1)	55.2	46.1	54.6	31.6	64.9	43.5	34.1
SFT	C	750M	27.6 (30.1)	31.8 (34.6)	18.2 (11.2)	46.7 (48.0)	24.2 (27.4)	51.9 (57.1)	38.5 (42.5)	9.7 (7.6)	29.9 (32.2)	0.0 (0.0)	31.2 (22.9)	55.3	46.1	54.3	30.2	65.6	37.5	30.3
KD	C	250M	37.9 (39.9)	41.6 (42.1)	36.2 (36.0)	48.9 (48.6)	35.4 (36.6)	65.6 (67.6)	48.8 (50.2)	20.5 (20.8)	35.8 (37.8)	18.3 (24.4)	44.7 (41.6)	56.4	44.9	54.9	31.7	65.2	40.6	37.7
KD	C	500M	39.9 (40.9)	40.7 (41.3)	38.2 (39.0)	48.1 (49.4)	33.9 (35.0)	64.1 (65.8)	50.0 (50.6)	22.4 (22.5)	39.8 (40.3)	21.9 (22.6)	47.5 (42.9)	55.8	45.0	54.8	31.1	65.1	36.5	39.2
KD	C	750M	41.0 (41.0)	39.0 (40.9)	39.2 (39.7)	49.4 (49.6)	32.3 (33.4)	62.3 (63.4)	47.0 (49.7)	22.4 (22.9)	37.9 (39.4)	25.0 (21.9)	49.0 (44.0)	56.3	45.0	54.9	32.3	65.0	37.1	39.1

J Perplexity-Based Architecture Comparison

Table 2 in the main text reports generation-based results. Here we present the corresponding perplexity-based (LM Evaluation Harness) results for the same five architectures.

Table 19: Architecture comparison under perplexity-based evaluation (LM Evaluation Harness). Same models as Table 2. We report accuracy (%) for all tasks except LAMBADA, where we report perplexity (↓). Best student result per column in **bold**. BBH, GSM8K, and IFEval are excluded: all models score $\leq 1.4\%$ under likelihood-based scoring, likely reflecting task format incompatibility rather than meaningful model differences.

Model	WG ↑	HS ↑	ARC-E ↑	ARC-C ↑	PIQA ↑	LAM. ↓	MMLU ↑	CMMLU ↑
<i>Teacher (Qwen3-0.6B)</i>	55.5	47.3	55.6	34.2	65.9	24.7	40.2	— [†]
Pure KDA	55.1	42.9	49.5	29.4	64.3	53.7	35.9	33.3
Pure Mamba	53.8	39.2	39.8	26.4	63.3	135.0	25.0	26.4
Hybrid Mamba	54.0	42.9	53.6	30.5	65.7	73.0	34.7	38.8
Hybrid KDA	57.2	45.2	52.5	31.7	66.3	38.0	40.6	40.0

[†]Teacher CMMLU not evaluated under LM-Eval.

Architecture rankings under perplexity-based evaluation are broadly consistent with generation-based results: Hybrid KDA leads on most metrics and Pure Mamba is weakest. However, inter-model differences are markedly compressed: PPL-based scoring narrows the architecture gaps substantially compared to generation-based evaluation, with the exception of Pure Mamba’s catastrophic LAMBADA perplexity. This reinforces the paper’s central finding that perplexity-based metrics underestimate quality differences between architectures.

K Maximum Throughput Under GPU Saturation

The batch-size-1 measurements in Section 6.1.1 do not capture the primary deployment benefit of reduced KV cache memory: fitting larger batches. Figure 5 reports peak throughput at each context length by sweeping batch sizes up to OOM.

At short contexts (2K), KV cache memory is small relative to model weights, so all architectures achieve similar peak throughput. As context length grows, KV cache dominates memory allocation for the Transformer, limiting its maximum batch size. The SSM and hybrid variants, with $\sim 75\%$ smaller cache, sustain larger batches and achieve up to $5\times$ higher peak throughput at 128K tokens.

L Long-Context Quality

The efficiency gains reported in Section 6.1.1 are meaningful only if hybrid models preserve functional quality at long contexts. We evaluate on LongBench (Bai et al., 2024) (real-world QA and summarization, 8K–22K tokens) and RULER (Hsieh et al., 2024) (synthetic needle-in-a-haystack retrieval, 4K–128K tokens). Importantly, no dedicated long-context extension training was performed: all students were distilled on

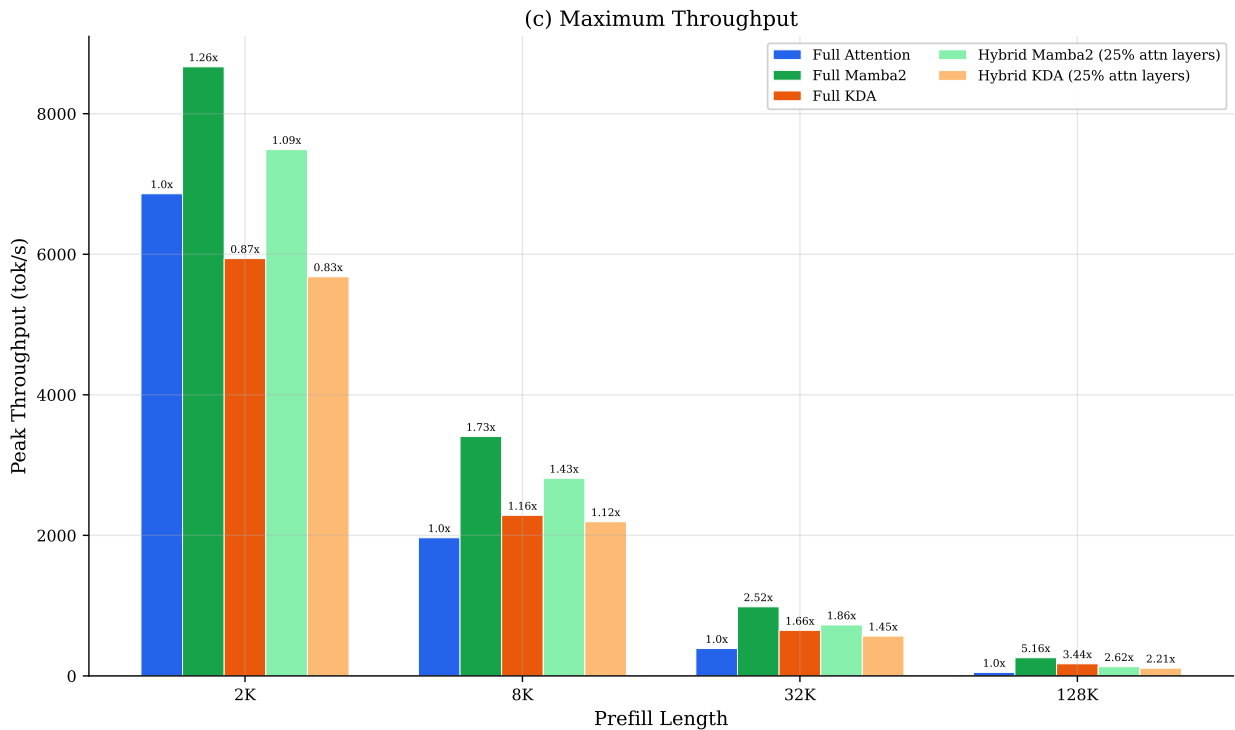


Figure 5: (a) Theoretical cache memory vs. sequence length. Attention cache grows linearly with context; SSM state is constant. (b) Peak throughput (sweeping batch size to OOM) at four context lengths. Annotations show relative throughput vs. the Teacher. At 32K+ tokens, SSM variants achieve 1.9–2.5 \times the teacher’s peak throughput by fitting larger batches.

sequences of at most 4K tokens. The resulting gap relative to the teacher is therefore expected and could likely be narrowed with targeted long-context training (Chen et al., 2026).

Table 20: LongBench results (F1 or ROUGE, $\times 100$; contexts 8K–22K tokens). DuR = DuReader, HQA = HotpotQA, MuS = MuSiQue, NQA = NarrativeQA, QMS = QMSum, TQA = TriviaQA. “Hybrid” models retain 7 attention layers; “Pure” models use 0. Best student per column in **bold**.

Model	DuR	HQA	MuS	NQA	QMS	TQA	Avg
<i>Teacher (Qwen3-0.6B)</i>	32.8	24.4	8.6	13.0	21.0	59.6	26.6
Pure Mamba	4.4	0.6	0.6	0.9	9.7	1.9	3.0
Pure KDA	16.1	7.6	3.3	9.3	19.4	19.9	12.6
Hybrid Mamba	21.5	10.8	3.0	6.6	15.5	26.6	14.0
Hybrid KDA	21.4	12.5	5.2	10.3	18.6	19.1	14.5

On LongBench (Table 20), all students fall substantially short of the teacher. The architecture hierarchy mirrors the short-context results (Table 2): Pure Mamba collapses (Avg 3.0), Pure KDA is moderate (12.6), and both hybrid variants lead, with Hybrid KDA (14.5) narrowly ahead of Hybrid Mamba (14.0). Individual task rankings vary (Hybrid Mamba leads on DuReader and TriviaQA, while Hybrid KDA is stronger on HotpotQA, MuSiQue, and NarrativeQA), but the overall gap to the teacher remains large, underscoring that short-context distillation alone does not fully transfer long-range comprehension.

The NIAH results (Table 21) provide a finer-grained view. Pure Mamba fails completely across all needle types and context lengths (0.0%), confirming that Mamba2 layers lack the precise token-level retrieval mechanism required for needle-in-a-haystack tasks. Pure KDA retains some retrieval ability on the simplest

Table 21: RULER NIAH single-needle retrieval accuracy (%) across context lengths. The three Single variants differ in haystack complexity and needle value type: **Single-1** embeds a numeric needle in a short repeated sentence, **Single-2** embeds a numeric needle in natural prose (Paul Graham essays), and **Single-3** embeds a UUID string in the same natural prose. “Hybrid” models retain 7 attention layers; “Pure” models use 0. Best student per column in **bold**.

Model	NIAH-Single-1						NIAH-Single-2						NIAH-Single-3					
	4K	8K	16K	32K	64K	128K	4K	8K	16K	32K	64K	128K	4K	8K	16K	32K	64K	128K
<i>Teacher</i>	100.0	100.0	100.0	100.0	100.0	0.0 [†]	100.0	100.0	100.0	100.0	99.4	0.0 [†]	99.4	99.8	100.0	100.0	78.8	0.0 [†]
Pure Mamba	0.0	0.0	0.0	0.0	0.0	0.0	0.0	0.0	0.0	0.0	0.0	0.0	0.0	0.0	0.0	0.0	0.0	0.0
Pure KDA	96.4	88.8	60.2	29.0	11.2	5.4	0.6	0.0	0.0	0.0	0.0	0.0	0.0	0.0	0.0	0.0	0.0	0.0
Hybrid Mamba	100.0	100.0	100.0	97.6	75.8	14.0	100.0	100.0	95.8	37.6	4.2	1.0	86.8	74.6	25.2	14.8	3.2	0.0
Hybrid KDA	99.2	100.0	98.8	94.8	92.6	43.0	99.0	99.8	98.6	58.4	26.4	2.4	80.2	82.0	58.0	19.6	5.6	0.0

[†]Qwen3-0.6B supports up to 40K positions; 128K results are out-of-distribution.

needle type (Single-1: 96.4% at 4K) but collapses to near-zero on Single-2 (0.6%) and Single-3 (0.0%). The dramatic difference is explained by the task structure: in Single-1, the haystack is a short sentence repeated many times, making any inserted needle highly salient against a trivially predictable background; in Single-2/3, the needle must be located within coherent natural prose, requiring precise positional attention that linear sequence mixers fundamentally lack. Single-3 adds further difficulty by requiring exact reproduction of 36-character UUID strings rather than short numbers, a task that demands character-level fidelity from the retrieval mechanism. This progression exposes a fundamental limitation of KDA layers: their success on Single-1 reflects pattern-matching against a predictable context rather than genuine retrieval capability. Both hybrid models perform dramatically better, with near-perfect accuracy on Single-1 and Single-2 at short contexts. Hybrid Mamba slightly outperforms Hybrid KDA at short contexts on the easiest tasks, but Hybrid KDA degrades more gracefully at longer contexts, maintaining 92.6% at 64K on Single-1 versus 75.8% for Hybrid Mamba. On the hardest needle type (Single-3), both hybrid models struggle beyond 16K tokens, with Hybrid KDA retaining a slight edge at 8K–32K.

Taken together, the long-context results confirm that hybrid architectures enable meaningful efficiency gains (Section 6.1.1) while retaining basic retrieval capability. Retained attention layers are essential for non-trivial retrieval, with both pure architectures failing on harder needle types. Among hybrid variants, KDA maintains a slight overall edge, particularly at longer contexts. Nevertheless, a substantial quality gap to the teacher persists, especially for harder retrieval patterns and longer contexts. Closing this gap through dedicated long-context training (Chen et al., 2026) is a natural direction for future work.